
Insertion Based Sequence Generation with Learnable Order Dynamics

Dhruvsh Patel^{*1} Benjamin Rozonoyer^{*1} Gaurav Pandey² Tahira Naseem² Ramón Fernandez Astudillo²
Andrew McCallum¹

 Project  Code

Abstract

In many domains generating variable length sequences through insertions provides greater flexibility over autoregressive models. However, the action space of insertion models is much larger than that of autoregressive models (ARMs) making the learning challenging. To address this, we incorporate trainable order dynamics into the target rates for discrete flow matching, and show that with suitable choices of parameterizations, joint training of the target order dynamics and the generator is tractable without the need for numerical simulation. As the generative insertion model, we use a variable length masked diffusion model, which generates by inserting and filling mask tokens. On graph traversal tasks for which a locally optimal insertion order is known, we explore the choices of parameterization empirically and demonstrate the trade-offs between flexibility, training stability and generation quality. On *De Novo* small molecule generation, we find that the learned order dynamics leads to an increase in the number of valid molecules generated, when compared to uniform order dynamics.

1. Introduction

The dilemma of *which substructures to generate in what order* is highly pronounced for the generative modeling of discrete data. Autoregressive models generate sequences in a fixed left-to-right order, which is not suitable for many applications where the dependencies in the tokens is more global (Valmeekam et al., 2023; Bachmann & Nagarajan, 2024; Dziri et al., 2023; Lee et al., 2025). In contrast, non-autoregressive models like Masked Diffusion models (MDMs) (Sahoo et al., 2024b; Shi et al., 2024) and Discrete Flow Matching (DFMs) (Campbell et al., 2024; Gat

et al., 2024) learn to generate sequences in arbitrary order. While this provides flexibility, it also makes the learning difficult (Kim et al., 2025b). Specifically, the use of absolute position information and fixed length assumption does not allow the generator to exploit token dependencies that are better expressed in terms of pairwise relative positions (Patel et al., 2025a; Huang et al., 2026). Therefore, learning a good generation order also has limited benefits in the context of fixed length unmasking models like MDMs.

To overcome the limitations of fixed length unmasking, several insertion based variable length generative models have been proposed wherein the sequence is generated by inserting tokens (Havasi et al., 2025; Patel et al., 2025b). This allows for flexible generation order, while also taking advantage of relative position based token dependencies. However, purely insertion based models forgo the parallel generation benefits of unmasking models. Kim et al. (2025a) proposes FlexMDM, a variable length masked DFM, which combines the benefits of insertion and unmasking based models. FlexMDM unmask existing tokens and simultaneously inserts new mask tokens in an interleaved manner. However, the action space of FlexMDM is much larger than that of MDMs. This added expressivity makes learning challenging.

In this work, we leverage the flexibility of the DFM framework (Lipman et al., 2024a) to inject learnable parameters into the data sample dependent insertion and unmasking rates of FlexMDM, which have the effect of controlling the generation order while still maintaining the same terminal time distribution. By matching those target rates, the generator learns to generate in the order implicit in the target rates. We show that both the generator and the sample-dependent target rates can be learned simultaneously without the need for simulating the entire trajectory, and in fact using just a single backward pass of automatic differentiation per input sample. We call our method *LFlexMDM*, which is short for FlexMDM with *Learnable Order Dynamics*. Experiments on *de novo* molecule generation demonstrate that learned order dynamics lead to significant improvements in the validity and quality of generated samples compared to FlexMDM.

^{*}Equal contribution ¹University of Massachusetts Amherst ²IBM Research. Correspondence to: Dhruvsh Patel <dhruvshpate@umass.edu>.

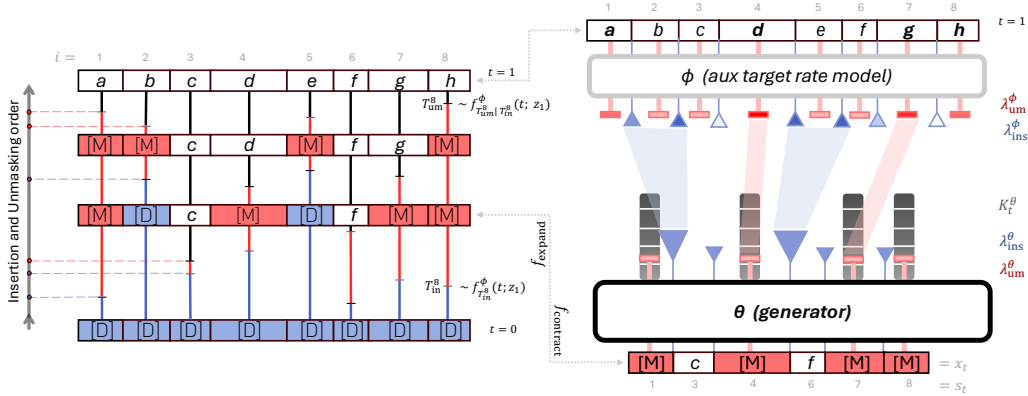


Figure 1. **Left:** Alignment-preserving data dependent generation process for variable-length sequence with learnable insertion and unmasking time schedules. The unmasking and insertion times induce a generation order. **Right:** The auxiliary neural network (top right) takes in a clean sequence x_1 , and outputs per-token target insertion rates λ_{in}^ϕ and unmasking rates λ_{um}^ϕ . The generator network (bottom right) takes in a partial sequence x_t and produces insertion $\lambda_{\text{in}}^\theta$ and unmasking $\lambda_{\text{um}}^\theta \cdot K^\theta$ rates to match the target rates.

2. Preliminaries: Discrete Flow Matching

Let \mathbb{X} be a countable space in which our data lives (e.g., the space of sequences of length L). The aim is to construct a generative process that samples from a desired distribution $p_1 = p_{\text{data}}$ over this space. Discrete Flow Matching (Campbell et al., 2024; Gat et al., 2024) constructs a continuous time Markov chain $\{X_t\}$ taking values in \mathbb{X} , with time marginals $p_t(x) := \mathbb{P}(X_t = x)$, which transforms an initial sample $X_0 \sim p_0$ to a final sample $X_1 \sim p_1 = p_{\text{data}}$, where p_0 is easy to sample from. For small time steps h , the CTMC transitions follow $x_{t+h} \sim p_{t+h|t}(\cdot | x_t) := \mathbb{P}(X_{t+h} = \cdot | X_t = x_t)$, where the transition probability is given by

$$p_{t+h|t}(y | x) = \delta_x(y) + h R_t(x, y) + o(h), \quad (1)$$

and $\delta_x(y)$ is the indicator function. The initial distribution p_0 and the rate R_t of the CTMC determine the generative process completely.¹ Therefore, to obtain the desired CTMC, one first constructs a probability flow p_t such that the desired terminal distribution condition is satisfied: $p_{t=1} = p_{\text{data}}$, and then constructs a (non-unique) generator rate R_t that satisfies the Kolmogorov Forward Equation:

$$\partial_t p_t(x) = \sum_{y \in \mathbb{X}} R_t(y, x) p_t(y). \quad (2)$$

Such a rate is said to *generate* the marginal probability path p_t . The general template is to choose a family of densities $p_{t|C}$, where $C \in \mathbb{C}$ is an indexing or conditioning variable, typically an endpoint pin $C = (X_0, X_1)$, and then to match the unknown rates $R_t^\theta(x, \cdot)$ with the target conditional rates $R_t(x, \cdot | C)$ that generate $p_{t|C}$ (in the sense of Equation (2)) by minimizing the Bregman divergence:

$$\mathcal{L}(\theta) = \mathbb{E}_{X_t, C} D(R_t(X_t, \cdot | C), R_t^\theta(X_t, \cdot)), \quad (3)$$

¹Please refer to Section B for an extended discussion.

where the expectation is over $C \sim p(C)$, $X_t \sim p_{t|C}$. In the case of $C = (X_0, X_1)$, where $X_1 \sim p_{\text{data}}$, this minimizes a lower bound on the data log-likelihood (Shaul et al., 2025).

Projected DFM: The framework of DFM can be generalized to construct a conditional rate on an auxiliary space \mathbb{Z} , where it may be easier to define the dynamics, and then *project* the rate onto the space of interest \mathbb{X} creating weakly intertwined CTMCs as shown in the schematic in Figure 2.² Let $\{Z_t\}$ be a CTMC taking values in \mathbb{Z} , and define $\pi_{\text{enc}}(x | z)$ to be an *encoder kernel* from \mathbb{Z} to \mathbb{X} , then the auxiliary dynamics induce a (law-dependent) projected CTMC on \mathbb{X} with rate

$$R_t^\pi(x, y) = \sum_{z, w \in \mathbb{Z}} \pi_{\text{enc}}(y | w) \pi_{\text{dec}, t}(z | x) R_t(z, w), \quad (4)$$

where $z, w \in \mathbb{Z}$, R_t is the rate for the CTMC $\{Z_t\}$, and $\pi_{\text{dec}, t}(z | x) \propto p_t(z) \pi_{\text{enc}}(x | z)$ is the Bayes decoder. The same construction applies to conditional rates $R_t(z, w | C)$, yielding projected conditional rates $R_t^\pi(x, y | C)$. Even though the target path is defined through the auxiliary process, we can still learn the generator R_t^θ over \mathbb{X} alone by minimizing the Bregman divergence:

$$\mathcal{L}(\theta) = \mathbb{E}_{X_t, C} D(R_t^\pi(X_t, \cdot | C), R_t^\theta(X_t, \cdot)), \quad (5)$$

where the expectation is again over $C \sim p(C)$, $X_t \sim p_{X_t|C}$.

²This is a slight generalization of (Havasi et al., 2025; Kim et al., 2025a). See Section C for the discussion.

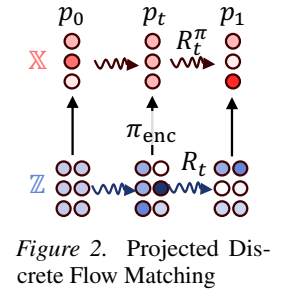


Figure 2. Projected Discrete Flow Matching

Positional Independence Assumption. For product spaces \mathbb{X}^L like the space of sequences, the size of the general rate matrix grows exponentially with the length L . To avoid this, sparsity is introduced into the rate matrix by assuming per-position independence of the target conditional probability $p_{t|C}(x_t|c)$, i.e., $p_{t|C}(x_t|c) = \prod_{i=1}^L p_{t|C}^i(x_t^i|c)$, where the superscript i denotes the i -th position, which results in the corresponding rate matrix being a mixture of per-position rates (Campbell et al., 2022):

$$R_t(x, y|C) = \sum_{i=1}^L \delta_{x^{-i}}(y^{-i}) R_t^i(x, \text{sub}(x, i, y^i) | C),$$

where $\text{sub}(x, i, y^i)$ denotes the sequence obtained by replacing the token at i -position in x with y^i , and x^{-i} denotes the sequence x , with the i -th position excluded. We will use $R_t^i(x, y^i|C)$ to denote $R_t(x, \text{sub}(x, i, y^i) | C)$ compactly.

3. Variable Length Sequence Generation

Let $\mathbb{X} := \bigcup_{k=1}^L \mathbb{V}^k$ the space of variable length sequences. Since there are multiple possible alignments of a partial sequence x_t to a clean sequence x_1 , it is not easy to construct conditional marginals $p_{t|C}(x_t|x_1)$ as is typically done in masked DFM (Campbell et al., 2024; Gat et al., 2024). However, one can use an auxiliary space that include the alignment information and perform projected rate matching. Similarly to Kim et al. (2025a), we define the auxiliary space of partial sequences as $\mathbb{Z} := \bigcup_{k \in [L]} \mathbb{V}^k \times \mathbb{S}_k$, where $\mathbb{S}_k := \{(s^1, \dots, s^k) \in [L]^k \mid s^1 < \dots < s^k\}$ is the space of ordered tuples of positions and L is the maximum length. An example element of \mathbb{Z} is shown on the right of Figure 1 as the input (x_t, s_t) to the generator. Additionally, we note a useful isomorphism. Let $[\text{D}]$ be a special token outside the vocabulary \mathbb{V} that is used to indicate a dropped position. Then $\bar{\mathbb{Z}} := (\mathbb{V} \cup \{[\text{D}]\})^L$ is isomorphic to \mathbb{Z} through the mapping $f_{\text{contract}} : \bar{\mathbb{Z}} \rightarrow \mathbb{Z}$ that removes the $[\text{D}]$ tokens from the \bar{z} to form x , and moves the exact position information to s to produce $z = (x, s)$. For example, as shown in Figure 1, for $L = 8$ and $\bar{z} = ([\text{M}], [\text{D}], c, [\text{M}], [\text{D}], f, [\text{M}], [\text{M}])$, $f_{\text{contract}}(\bar{z}) = (([\text{M}], c, [\text{M}], f, [\text{M}], [\text{M}]), (1, 3, 4, 6, 7, 8))$. From this point on, we will use z to mean an element of \mathbb{Z} or $\bar{\mathbb{Z}}$ interchangeably. Finally, we denote $f_{\text{rm-drop}} : \bar{\mathbb{Z}} \rightarrow \mathbb{X}$ to be the function that removes the exact position to produce a sequence in the original space, i.e., for our previous example, $f_{\text{rm-drop}}(\bar{z}) = (a, b, c)$.

Mixture paths in the auxiliary space. We construct mixture paths on $\bar{\mathbb{Z}}$ by setting the conditioning variable as (z_1, z_0) , where $z_1 = (x_1 \odot [\text{D}]^{L-\text{len}(x_1)} [\text{D}], [L])$ and $z_0 = [\text{D}]^L [\text{D}]$, with \odot denoting the sequence concatenation operation. The goal is to define per-position target

rates such that the transition $[\text{D}] \rightarrow [\text{M}] \rightarrow z_1^i$ occurs for each position i where $z_1^i \neq [\text{D}]$ such that we can express a tractable distribution over the orderings of insertion and unmasking events for the entire sequence, which can be learned along with the generator parameters.

3.1. Learnable Order Dynamics

Any regular CTMC over countable state space can be represented using a Poisson process and an embedded state transition kernel. Therefore, we define the per-position target rates as

$$R_t^i(z, w^i | (z_1, z_0)) = \lambda_t^i(z; (z_1, z_0)) \cdot K_t^i(z, w^i | (z_1, z_0)),$$

where $\lambda_t^i(z; (z_1, z_0))$ is the state and time dependent arrival rate of the Poisson process, and $K_t^i(z, w^i | (z_1, z_0))$ is the state transition kernel, i.e., when an arrival occurs at the i -th position, the state changes according to the categorical distribution K_t^i . In order for $R_t(z, w)$ to be a valid rate, $\lambda_t^i > 0$ and $K_t^i(z, z^i) = 0$. This characterization allows us to express the order dynamics by controlling the hazard rates, without changing the terminal state distributions of the process. For our case of two events per position, **insertion** and **unmasking**, we denote the respective event times as $T_{\text{in}}^i := T_1^i$ and $T_{\text{um}}^i := T_2^i$. The left side of Figure 1 provides an intuitive illustration of the induced order dynamics. Proposition 1 shows that the target rates that generate the desired conditional probability flow can be expressed using two increasing right continuous functions. Note that since $z_0 = [\text{D}]^L [\text{D}]$ is fixed, we will hide the dependence on z_0 from the notation for brevity.

Proposition 1 (Target conditional rates). *Let $\mathbb{P}(T_{\text{in}}^i \leq t) = F_{\text{in}}^i(t)$ and $\mathbb{P}(T_{\text{um}}^i \leq t \mid T_{\text{in}}^i = s) = \delta(t \geq s) \frac{F_{\text{um}}^i(t) - F_{\text{um}}^i(s)}{1 - F_{\text{um}}^i(s)}$, where $F_{\text{in}}^i(t)$ and $F_{\text{um}}^i(t)$ are right continuous and non-decreasing functions on $[0, 1]$ with $F_{\text{in}}^i(0), F_{\text{um}}^i(0) = (0, 0)$, and $F_{\text{in}}^i(1), F_{\text{um}}^i(1) = (1, 1)$. Then the rate*

$$\lambda_t^i(z; z_1) = \begin{cases} \frac{\dot{F}_{\text{in}}^i(t; z_1)}{1 - F_{\text{in}}^i(t; z_1)} & \text{if } z^i = [\text{D}] \neq z_1^i, \\ \frac{\dot{F}_{\text{um}}^i(t; z_1)}{1 - F_{\text{um}}^i(t; z_1)} & \text{if } z^i = [\text{M}], \\ 0 & \text{otherwise.} \end{cases} \quad (6)$$

$$K_t^i(z, w^i | z_1) = \begin{cases} \delta_{[\text{M}]}(w^i) & \text{if } w^i = [\text{D}], \\ \delta_{z_1^i}(w^i) & \text{if } w^i = [\text{M}], \\ \text{undefined} & \text{otherwise.} \end{cases} \quad (7)$$

generates the marginals (i.e., satisfies the KFE):

$$\begin{aligned} & p_t^i(z^i | z_1) \\ &= \begin{cases} \mathbb{P}(T_{\text{in}}^i > t) \delta_{[\text{D}]}(z^i) & \text{if } z_1^i \neq [\text{D}], \\ \quad + \mathbb{P}(T_{\text{in}}^i \leq t < T_{\text{um}}^i) \delta_{[\text{M}]}(z^i) \\ \quad + \mathbb{P}(T_{\text{um}}^i \leq t) \delta_{z_1^i}(z^i) & \\ \delta_{[\text{D}]}(z^i) & \text{if } z_1^i = [\text{D}], \end{cases} \end{aligned} \quad (8)$$

and these marginals satisfy the boundary conditions $p_1^i(z^i|z_1) = \delta_{z_1^i}(z^i)$ and $p_0^i(z^i|z_1) = \delta_{[D]}(z^i)$.

3.1.1. PARAMETERIZATION

By learning the parameters ϕ governing $F_*^{\phi,i} : [0, 1] \times \mathbb{Z} \rightarrow [0, 1]$ of Proposition 1 we can learn the target order dynamics. The choice of the functional form of F_* depends on the analytical tractability of the resulting $p_t^\phi(z|z_1)$. Specifically, we need to be able to sample $z_t \sim p_t^\phi(z|z_1)$ (ideally using inverse CDF sampling) in order to compute the projected rate matching loss (Equation (5)) and also be able to compute the likelihood $p_t^\phi(z|z_1)$ for updating ϕ , ideally in closed form to avoid numerical integration. Note that since the likelihood is independent per-position, if we satisfy the desiderata stated above, we obtain an efficient training procedure as discussed in Section 3.2. As discussed in Appendix D.2, the likelihood $p_t^\phi(z|z_1)$ requires computing the following integral:

$$\mathbb{P}(T_{\text{in}}^i \leq t < T_{\text{um}}^i) = (1 - F_{\text{um}}^i(t)) \int_0^t \frac{\dot{F}_{\text{in}}^i(s)}{1 - F_{\text{um}}^i(s)} ds.$$

The Kumaraswamy CDF (Kumaraswamy, 1980) (shown in Figure 3):

$$F_*^{\phi,i}(t; z_1) = 1 - (1 - t^{a_*})^{b_*}, \quad * \in \{\text{in}, \text{um}\} \quad (9)$$

is an ideal candidate for the functional form of F_* as it allows inverse CDF sampling, can produce internal modes, and for $a_{\text{in}}^i = a_{\text{um}}^i = a$, allows us to obtain closed form expressions for the likelihood (see Appendix D.5.3 for more details). Therefore, we parameterize $b_{\text{in}}^{\phi,i}(z_1)$ and $b_{\text{um}}^{\phi,i}(z_1)$ by a transformer with weights represented by ϕ , and set $a_{\text{in}}^i = a_{\text{um}}^i = a$ to be a constant, which yields the following closed form expressions for the hazard rates:

$$\lambda_{\text{in}}^i(t) = b_{\text{in}} \frac{at^{a-1}}{1-t^a}, \quad \lambda_{\text{um}}^i(t) = b_{\text{um}} \frac{at^{a-1}}{1-t^a}. \quad (10)$$

Interestingly, in this final form, we can see that the shape function $\frac{at^{a-1}}{1-t^a}$ is the same for both insertion and unmasking, and only the hazard rate multipliers b_{in} and b_{um} control the overall rate. Under the time-change $\tau = -\log(1 - t^a)$, it becomes an exponential race with the parameters b_{in} and b_{um} with precedence constraints (insertion before unmasking).

3.2. Training

The training objective, illustrated on the right side of Figure 1 can be derived using projected rate matching (Ap-

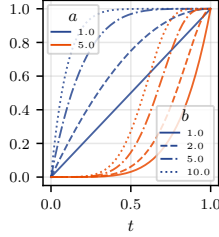


Figure 3. Kumaraswamy CDF shapes for different parameter values.

pendix C.0.1), and is given by the unmasking and insertion loss as follows:

$$\mathcal{L}_{\text{um}}^{\phi,\theta} = \mathbb{E}_{\phi} \left[\sum_{i=1}^{\text{len}(x_t)} \delta_{[M]}(x_t^i) \left(-\lambda_{\text{um},t}^{\phi,s_t^i}(z_1) \log K_t^{\theta,i}(z_1^{s_t^i}|x_t) + D_{\psi}(\lambda_{\text{um},t}^{\phi,s_t^i}(z_1), \lambda_{\text{um},t}^{\theta,i}(x_t)) \right) \right], \quad (11)$$

$$\mathcal{L}_{\text{in}}^{\phi,\theta} = \mathbb{E}_{\phi} \left[\sum_{i=0}^{\text{len}(x_t)} D_{\psi} \left(\sum_{j \in \text{gap}_i(s_t)} \lambda_{\text{in},t}^{\phi,j}(z_1), \lambda_{\text{in},t}^{\theta,i}(x_t) \right) \right],$$

where the expectation is over $t \sim \mathcal{U}(0, 1)$, $z_1 \sim p_{\text{data}}$, $z_t \sim p_{t|z_1}^{\phi}$, and $x_t = f_{\text{rm-drop}}(z_t)$. The Bregman divergence D_{ψ} is computed using the negative entropy function $\psi(r) = -\sum_k r_k \log r_k$. We provide a step-by-step derivation of the training objective in Appendix D.4. Furthermore, Proposition 5 in Appendix C.0.1 shows that using the standard argument of using KL-divergence between CTMC path measures, followed by the data processing inequality, this loss maximizes a lower bound on the data log-likelihood under the generator.

Remark 1. For the case of fixed ϕ such that $a_*^{i,\phi} = b_*^{i,\phi} = 1$ for all i , the Bregman divergence $D(\lambda_{\text{um}}^{\phi}, \lambda_{\text{um}}^{\theta})$ becomes zero, and we obtain the loss equivalent to FlexMDM (Kim et al., 2025a) written in terms of rates instead of posterior probabilities. Therefore, we call our method LFlexMDM, where L stands for learnable order dynamics.

Remark 2 (Schedule regularization). Since both the generator and target rates are trainable, they can take extreme values creating numerical degeneracy in the training. To discourage such degenerate schedules, we add a schedule regularization term as described in Appendix D.5.2.

3.2.1. GRADIENT COMPUTATION

Since the expectation depends on the target rate network parameters ϕ , we resort to score based gradient estimation for ϕ and use REINFORCE leave-one-out (Kool et al., 2019) to reduce variance with minimal impact on training efficiency. The estimator for $\nabla_{(\phi,\theta)} \mathbb{E}[\mathcal{L}^{\phi,\theta}]$ is

$$\begin{aligned} & \frac{1}{2} \left[\mathcal{L}^{\phi,\theta}(z^{(1)}) - \mathcal{L}^{\phi,\theta}(z^{(2)}) \right] \left[\nabla_{\phi} \log \frac{p_{t|z_1}^{\phi}(z^{(1)})}{p_{t|z_1}^{\phi}(z^{(2)})} \right] \\ & + \frac{1}{2} \left[\nabla_{\phi} \mathcal{L}^{\phi,\theta}(z^{(1)}) + \nabla_{\phi} \mathcal{L}^{\phi,\theta}(z^{(2)}) \right] \\ & \frac{1}{2} \left[\nabla_{\theta} \mathcal{L}^{\phi,\theta}(z^{(1)}) + \nabla_{\theta} \mathcal{L}^{\phi,\theta}(z^{(2)}) \right], \end{aligned} \quad (12)$$

where $z^{(1)}, z^{(2)} \sim p_{t|z_1}^{\phi}$ and $z_1 \sim p_{\text{data}}$ (see Appendix D.5 for the details). We perform the gradient updates using a single backward pass of autograd using the stop-gradient (sg) operator as shown in Algorithm 1.

Algorithm 1 Training for LFlexMDM

Require: Dataset \mathcal{D} , generator parameters θ , target rate parameters ϕ , learning rate η

- 1: **while** not converged **do**
- 2: Sample $z_1 \sim p_{\text{data}}$ and $t \sim \mathcal{U}(0, 1)$
- 3: Compute $(a^{\phi,i}, b^{\phi,i}) \leftarrow \phi(z_1)$ for all $i \in \llbracket L \rrbracket$
- 4: **for** $k = 1$ to 2 **do**
- 5: Sample $T_{\text{in}}^{i,(k)} \sim F_{\text{in}}^{\phi,i}, T_{\text{um}}^{i,(k)} \leftarrow \text{TRUNC_SAMPLE}(T_{\text{in}}^{i,(k)}, F_{\text{um}}^{\phi,i})$
- 6: $z_t^{i,(k)} \leftarrow \begin{cases} [\text{D}] & T_{\text{in}}^{i,(k)} > t \\ [\text{M}] & T_{\text{in}}^{i,(k)} \leq t < T_{\text{um}}^{i,(k)} \\ z_1^i & \text{otherwise} \end{cases}$
- 7: $x_t^{(k)}, s_t^{(k)} \leftarrow f_{\text{contract}}(z_t^{(k)})$
- 8: $\mathcal{L}_k \leftarrow \mathcal{L}^{\phi,\theta}(x_t^{(k)}, s_t^{(k)}, z_1)$
- 9: **end for**
- 10: $\mathcal{L} \leftarrow \frac{1}{2} \left[(\text{sg}(\mathcal{L}_1) - \text{sg}(\mathcal{L}_2)) \log \frac{p_{t|z_1}^{\phi}(z_t^{(1)})}{p_{t|z_1}^{\phi}(z_t^{(2)})} + \mathcal{L}_1 + \mathcal{L}_2 \right]$
- 11: Update $(\theta, \phi) \leftarrow (\theta, \phi) - \eta \nabla_{(\theta,\phi)}^{\text{auto-grad}} \mathcal{L}$
- 12: **end while**

3.3. Sampling

As shown in Figure 1 on the bottom right, generator network predicts the rates $\lambda_{\text{in},t}^{\theta,i}(x_t)$ for insertion at gap position i and $\lambda_{\text{um},t}^{\theta,i}(x_t) K^{\theta,i}(\cdot|x_t)$ for unmasking at masked position i . We use a simple τ -leaping sampler (Gillespie, 2001) that allows to sample multiple events simultaneously. Additionally, the guarantee for the correctness of adaptive sampling from FlexMDM (Kim et al., 2025a) extends to LFlexMDM. The complete sampling algorithm is shown in Algorithm 2.

4. Related Work

For discrete diffusion, there exist different *fixed* noising processes like uniform noising, masking, or a mixture of both (Sahoo et al., 2024b; Schiff et al.; Zheng et al., 2025). For masked diffusion, Kim et al. (2025b) show that the order of denoising is crucial for the generative abilities of diffusion models, and the typical noising process that uses a uniform masking schedule may not be able to exploit the structure present in discrete sequences, thereby limiting the generators ability. Wang et al. (2025) looks at learning of generation order in any-order models (Hoogeboom et al., 2022; Uria et al., 2013), which have been shown to be equivalent to fixed length unmasking models (Ou et al., 2025). However, they work with the fixed length formulation using a Plackett-Luce model for the generation order.

The useful desiderata of *i*) modeling distributions over variable-length sequences and *ii*) the ability to insert tokens have inspired a number of recent works to move away from fixed-window text diffusion towards insertion- and

Algorithm 2 Tau-Leaping Sampling for LFlexMDM

- 1: **Input:** Time steps $0 = t_0 < t_1 < \dots < t_N = 1$, nucleus p , confidence function c
- 2: Initialize $x_0 = \emptyset$ (empty sequence)
- 3: **for** $n = 0$ to $N - 1$ **do**
- 4: $\tau \leftarrow t_{n+1} - t_n$
- 5: Predict $\lambda_{\text{in},t_n}^{\theta,i}(x_n), \lambda_{\text{um},t_n}^{\theta,i}(x_n)$, and $K^{\theta,i}(\cdot|x_n)$ from network θ
- 6: $x_{n+1} \leftarrow x_n$
- 7: **for** each gap position $i = 0$ to $\text{len}(x_n)$ **do**
- 8: $N_{\text{in}}^i \sim \text{Poisson}(\lambda_{\text{in},t_n}^{\theta,i}(x_n) \cdot \tau)$
- 9: **if** $N_{\text{in}}^i > 0$ **then**
- 10: Insert N_{in}^i masks at gap position i in x_{n+1}
- 11: **end if**
- 12: **end for**
- 13: **for** each masked position i in x_{n+1} **do**
- 14: **for** each token $y \in \mathbb{V}$ **do**
- 15: $N_{\text{um}}^{i,y} \sim \text{Poisson}(\lambda_{\text{um},t_n}^{\theta,i}(x_n) \cdot K^{\theta,i}(y|x_n) \cdot \tau)$
- 16: **end for**
- 17: //candidate unmask locations
- 18: $u_i \leftarrow \delta(\sum_{y \in \mathbb{V}} N_{\text{um}}^{i,y} > 0)$
- 19: **end for**
- 20: **if** confidence enabled **then**
- 21: // select $\{|i : u_i=1\}$ locations with largest confidence c_i
- 22: $u \leftarrow \text{SELECT}(\sum_i u_i; c(K^\theta, \lambda^\theta))$
- 23: **end if**
- 24: **for** each masked position i in x_{n+1} with $u_i = 1$ **do**
- 25: $x_{n+1}^{\text{nucleus}(p)} \sim K^{\theta,i}(\cdot|x_n)$
- 26: **end for**
- 27: **end for**
- 28: **return** x_N

substitution- based discrete flow models in which positions during the generation process acquire a relative rather than absolute interpretation. (Patel et al., 2025b) proposes Insertion Language Model (ILM) that generates sequences by jointly modeling the distribution over the insertion location and the vocabulary. Havasi et al. (2025) proposed EditFlows that uses the projected DFM to construct a generator CTMC that models the rates of insertion, deletion, and substitution operations. However, both these models can only insert one token per gap at a time. FlexMDM (Kim et al., 2025a) can insert multiple mask tokens per gap. But the flexibility comes at a cost. The action space of insertion based generation is larger than that of unmasking based models, and there have been limited attempts to explore learning the generation order in insertion based models. Most of the exiting works focus on models that insert one token at a time and require simulating the generation trajectory for learning the generation order (Gu et al., 2019; Brantley et al., 2019).

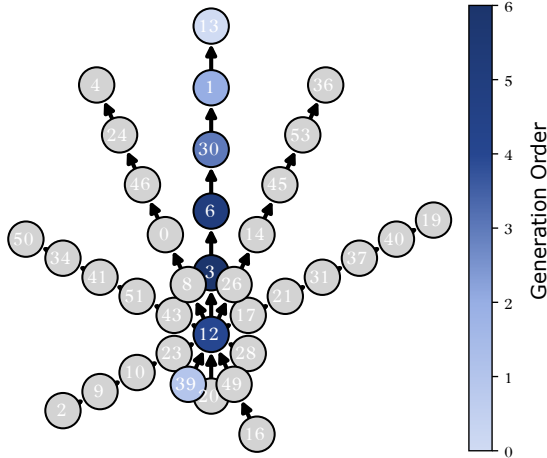


Figure 4. An example of generation trajectory of LFlexMDM shown as a traversal on the query graph. LFlexMDM learns to generate in local optimal order: starting from the end points of the arm and moving towards the junction.

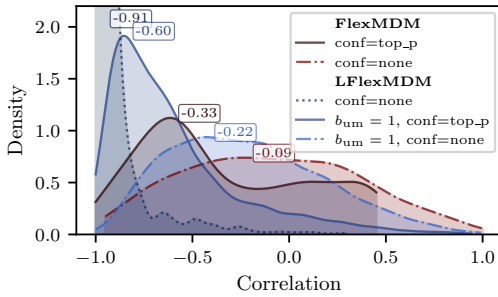


Figure 5. Correlation between generation order and distance from the junction node, both normalized by path length. Only examples that achieve 100% exact match are considered.

5. Experiments

Model. For all our experiments, we use DDiT (Lou et al., 2023) with RoPE, and adaptive layer-norm (AdaLN) for conditioning on the time variable (Peebles & Xie, 2023). We implement the target and generator rates with MLP scalar heads on top of the transformer. For FlexMDM (baseline), we follow the setup in Kim et al. (2025a), which also uses DDiT architecture, but has a length prediction head for insertion instead of a rate prediction head. We experiment with a “separate” setting where the target rates are predicted by a separate auxiliary transformer, and with a memory-efficient “shared” setting where all heads share the same backbone transformer, which is updated by both the ∇_{θ} and ∇_{ϕ} components of the Equation (12) gradient estimator.

Table 1. Exact Match (%) results for star graph traversal tasks. * indicates frozen, 🔥 indicates trainable; ✓/× indicate conf. enabled/disabled. We use top-1, i.e., $\arg \max(p)$ for sampling the tokens for all models.

	Model			Difficulty	
	b_{um}	b_{in}	conf.	medium	hard
1	ARM		N/A	75.0	23.0
2	MDM		✓	36.5	21.0
FlexMDM					
3	*	*	×	89.6	6.0
4	*	*	✓	91.3	7.4
LFlexMDM (Separate)					
5	🔥	🔥	×	92.3	38.0
6	*	🔥	×	93.2	87.9
7	*	🔥	✓	93.0	88.1
LFlexMDM (Shared)					
8	*	🔥	×	93.6	34.2
9	*	🔥	✓	93.2	69.7

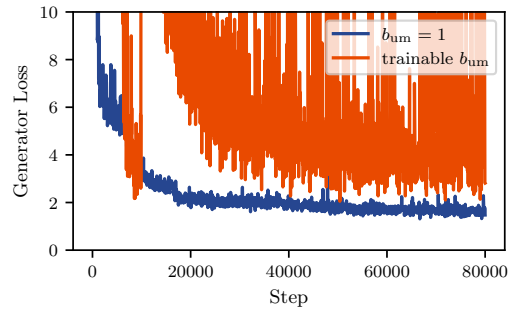


Figure 6. Loss comparison for the hard star graph traversal task with and without fixing target unmasking rate ($b_{um} = 1$). The erratic dynamics of a fully unconstrained set of target rates motivates freezing b_{um} .

5.1. Graph Traversal

Dataset. We use the star graphs dataset from Patel et al. (2025b).³ It consists of star shaped graphs with one junction node and multiple arms coming in and out of the junction node. The task is to produce a path from the given starting and terminal nodes. The input graph is stringified as edge pairs arranged in a random order (the order is random but remains fixed for a given graph). The input string is this stringified graph followed by the starting and terminal nodes, the model needs to generate the path (edges in the correct order) connecting the starting and terminal nodes. We use the medium and hard difficulty settings of the dataset as both of these use graphs with variable arm lengths. The graphs in the hard setting vary significantly in the number

³See Section E.1 for more details.

of arms as well as the arm lengths, making it a challenging task. However, if the edges of output path are generated starting from the end points moving towards the junction node, then the task becomes trivial even for a local model, i.e., a model that does not plan ahead.

5.1.1. DESIGN CHOICES

We use the graph traversal to explore the design choices for parameterizing the target hazard rates $\lambda_t^{\phi,i}(z; z_1)$.

Flexibility vs Stability: As noted in Section 3.1.1, the hazard rates have two free parameters for each position, b_{in}^i and b_{um}^i . We first examine the effect of flexibility of the target rate model $\lambda_t^{\phi,i}(z; z_1)$. Interestingly, the performance of the generator improves when the *unmasking* target rate b_{um} is fixed (❄) as opposed to trainable (🔥), as seen from the slight improvement in medium difficulty and a significant improvement in hard difficulty LFlexMDM (Table 1, line 5 vs line 6). Figure 9, which presents the loss comparison for the hard star graph traversal task with and without fixing target unmasking rate ($b_{um} = 1$), shows that the additional flexibility in learning b_{um} destabilizes the training.

Note that fixing b_{um} still leaves enough room for learning of insertion order, i.e., if $h_1 < h_2$, then for any t , $\mathbb{P}(T_{um} \leq t \mid T_{in} = h_1) < \mathbb{P}(T_{um} \leq t \mid T_{in} = h_2)$. The preference for unmasking orders will show up in $K_t^{\theta,i}$ values, which can be used for confidence-based position selection during decoding. Based on this observation, we fix $b_{um} = 1$ in the subsequent experiments.

Shared vs Separate Backbone: Additionally, we explore the use of a shared DDiT backbone for the target rate model and generator. For the hard version of the star graph traversal task, using a shared backbone leads to considerable drop in performance.

5.1.2. ANALYSIS: GENERATION ORDER

We also investigate whether the introduction of learnable target rates allows the generator to learn to generate the sequences in the optimal order. The optimal *local* order for star graphs starts from the end points of the arm and moves towards the junction. We analyze examples of the complete history of the generation under LFlexMDM and FlexMDM. As shown in the example in Figure 4, LFlexMDM indeed learns to generate in the optimal order. To inspect this further, we compute the correlation between the generation order and distance from the junction node. Since the arm lengths vary significantly for the hard version of the task, we normalize both the generation order and distance from the junction node by the path length. Figure 5 shows the correlation between the generation order (normalized by path length) and normalized distance from the junction node. The ideal correlation for optimal local order should be -1.

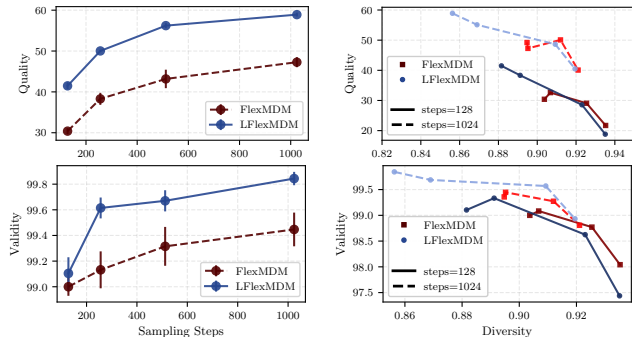


Figure 7. **Left:** Quality vs sampling steps for *de novo* generation for LFlexMDM and FlexMDM. **Right:** Quality vs diversity for *de novo* generation for LFlexMDM and FlexMDM.

Interestingly, we observe that LFlexMDM with trainable b_{um} (line 5 in Table 1) achieves mean correlation of -0.91 , when compared to -0.22 for the case when we fix $b_{um} = 1$ (line 6) and do not use confidence-based position selection during inference (line 7 in Table 1). Using confidence-based position selection for the fixed $b_{um} = 1$ case achieves a mean correlation of -0.60 . This supports our initial observation in Section 5.1.1 that fixing $b_{um} = 1$ stabilizes the training while still providing enough room for learning of ideal insertion order, which can be elicited even in the unmasking steps by confidence-based position selection. Interestingly, using confidence-based position selection for FlexMDM changes the correlation from -0.09 (light red) to -0.33 (dark red), lower than the respective correlation for LFlexMDM with fixed $b_{um} = 1$ (light blue to dark blue).

5.2. Small Molecule Generation

Dataset. We train all the models on the SAFE dataset (Noutahi et al., 2024), which consists of molecules from ZINC (Irwin et al., 2012) and UniChem (Chambers et al., 2013). Following Lee et al. (2025), we train for 50k steps with a global batch size of 2048. Based on the results of the graph traversal experiments, we fix the unmasking rate $b_{um}^{\phi} = b_{um}^{\theta} = 1$ and only keep the target insertion rate b_{in}^{ϕ} trainable. We evaluate on *de novo* generation by sampling 1000 molecules unconditionally from the trained models and compute the metrics of **validity**, **uniqueness**, **diversity**, and **quality**. Table 2 shows the results, and we provide a detailed analysis below.

Fixed window vs. variable length: For MDM, following Lee et al. (2025) we sample the lengths of the mask chunks from the ZINC250k distribution even for *de novo* generation. However, for FlexMDM and LFlexMDM, we perform completely unconstrained generation starting from a blank canvas. This highlights the advantage of working with a variable-length model.

Table 2. Results for *de novo* small molecule generation. For both FlexMDM and LFlexMDM, we use 1024 sampling steps. * indicates frozen, 🔥 indicates trainable; ✓/✗ indicates whether confidence-based position selection for unmasking is enabled, and p indicates the truncation threshold for nucleus sampling (Holtzman et al., 2020). † Noutahi et al. (2024) ‡ Lee et al. (2025)

Model				Validity (%)	Diversity	Uniqueness (%)	Quality (%)
b_{um}	b_{in}	conf.	p				
SAFE-GPT [†]				94.0 ±0.4	0.879 ±0.001	100.0 ±0.0	54.7 ±0.3
MDM [‡]				96.7 ±0.3	0.896 ±0.001	<u>99.3</u> ±0.2	53.8 ±1.7
FlexMDM							
*	*	×		98.9 ±0.4	0.922 ±0.001	96.4 ±0.3	39.5 ±1.6
*	*	✓		86.5 ±1.8	0.906 ±0.004	20.2 ±1.5	5.8 ±0.8
LFlexMDM (Aux. Size=medium)							
*	🔥	✓	1.0	98.9 ±0.2	<u>0.921</u> ±0.001	95.6 ±0.5	39.6 ±2.3
*	🔥	✓	0.5	99.7 ±0.1	0.870 ±0.002	88.6 ±0.5	54.7 ±1.7
*	🔥	✓	0.2	<u>99.8</u> ±0.1	0.857 ±0.001	86.1 ±0.7	59.2 ±1.1
*	🔥	×	1.0	99.0 ±0.2	<u>0.921</u> ±0.001	96.1 ±0.9	39.1 ±1.9
*	🔥	×	0.5	99.3 ±0.3	0.889 ±0.002	93.0 ±1.0	46.9 ±1.0
*	🔥	×	0.2	99.6 ±0.2	0.887 ±0.002	90.9 ±0.7	46.8 ±1.5
LFlexMDM (Aux. Size=small)							
*	🔥	✓	1.0	99.0 ±0.2	0.919 ±0.001	95.9 ±0.5	43.8 ±0.8
*	🔥	✓	0.5	99.7 ±0.1	0.837 ±0.003	82.6 ±0.7	52.4 ±1.7
*	🔥	✓	0.2	99.9 ±0.1	0.830 ±0.004	79.1 ±1.0	50.1 ±0.9
*	🔥	×	1.0	98.9 ±0.5	0.918 ±0.001	96.4 ±0.7	43.5 ±1.3
*	🔥	×	0.5	99.6 ±0.2	0.878 ±0.002	92.2 ±0.9	<u>61.2</u> ±1.8
*	🔥	×	0.2	99.5 ±0.2	0.864 ±0.002	87.2 ±1.3	62.1 ±1.7
LFlexMDM (Aux. Size=xtiny)							
*	🔥	✓	1.0	99.4 ±0.3	0.919 ±0.001	96.3 ±0.4	43.1 ±1.8
*	🔥	✓	0.5	99.7 ±0.1	0.851 ±0.003	87.8 ±1.2	60.0 ±0.4
*	🔥	✓	0.2	99.9 ±0.1	0.834 ±0.003	80.5 ±1.8	56.6 ±1.2
*	🔥	×	1.0	99.0 ±0.2	0.918 ±0.000	97.1 ±0.8	43.0 ±1.4
*	🔥	×	0.5	99.7 ±0.2	0.881 ±0.002	93.8 ±0.7	57.5 ±0.8
*	🔥	×	0.2	<u>99.8</u> ±0.1	0.876 ±0.002	90.3 ±1.5	58.9 ±1.2

Diversity-quality trade-off: As seen in Table 2, LFlexMDM shows improvement in validity and quality over FlexMDM, with a slight decrease in diversity. Indeed, this duality is expected because learning structurally good generation orders intuitively corresponds to reducing the randomness. Figure 7 (right) shows the plot of quality/validity vs. diversity as we vary the nucleus sampling p cut-off (Algorithm 2 line 25). We observe that LFlexMDM improves significantly in quality (~50% vs 60%) we reduce the randomness (lower p values) in the sampling process. In the same vein, uniqueness drops slightly, but validity improves, when we employ confidence-based position selection during decoding (lines 20-23), as opposed to sampling uniformly from eligible positions (line 18), making decoding more greedy.

Effect of inference budget: Next we fix the sampling parameters to their respective best values and vary the sampling steps. As seen in Figure 7 (left), **LFlexMDM shows consistent and significant improvement over FlexMDM**

in quality and validity at all sampling budgets.⁴

6. Conclusion

We introduce learnable order dynamics into variable-length unmasking DFM, allowing the model to learn to generate in favorable orders. By incorporating data-dependent insertion and unmasking rates, the model successfully learns task-specific optimal orders, when such an order exists, e.g. for graph traversal. The experiments on *de novo* molecule generation demonstrate that learned order dynamics lead to significant improvements in the validity and quality of generated samples compared to the baseline that does not use learned order dynamics.

Future Work: While the simultaneous simultaneous training of the generator and target rates using a single backward pass per example is relatively efficient, there is room for

⁴Results with additional nucleus-sampling p values, as well as a shared-backbone implementation, are provided in Table 7.

further improvement.

Impact Statement

This paper presents work whose goal is to advance the field of Machine Learning. There are many potential societal consequences of our work, none which we feel must be specifically highlighted here.

References

- Albergo, M. S., Boffi, N. M., and Vanden-Eijnden, E. Stochastic interpolants: A unifying framework for flows and diffusions. *arXiv preprint arXiv:2303.08797*, 2023.
- Bachmann, G. and Nagarajan, V. The pitfalls of next-token prediction. In Salakhutdinov, R., Kolter, Z., Heller, K., Weller, A., Oliver, N., Scarlett, J., and Berkenkamp, F. (eds.), *Proceedings of the 41st International Conference on Machine Learning*, volume 235 of *Proceedings of Machine Learning Research*, pp. 2296–2318. PMLR, 21–27 Jul 2024. URL <https://proceedings.mlr.press/v235/bachmann24a.html>.
- Bansal, A., Borgnia, E., Chu, H.-M., Li, J., Kazemi, H., Huang, F., Goldblum, M., Geiping, J., and Goldstein, T. Cold diffusion: Inverting arbitrary image transforms without noise. *Advances in Neural Information Processing Systems*, 36:41259–41282, 2023.
- Bartosh, G., Vetrov, D., and Naesseth, C. A. Neural flow diffusion models: Learnable forward process for improved diffusion modelling. *Advances in Neural Information Processing Systems*, 37:73952–73985, 2024.
- Brantley, K., Cho, K., Daumé, H., and Welleck, S. Non-monotonic sequential text generation. In Axelrod, A., Yang, D., Cunha, R., Shaikh, S., and Waseem, Z. (eds.), *Proceedings of the 2019 Workshop on Widening NLP*, pp. 57–59, Florence, Italy, August 2019. Association for Computational Linguistics. URL <https://aclanthology.org/W19-3620/>.
- Campbell, A., Benton, J., Bortoli, V. D., Rainforth, T., Deligiannidis, G., and Doucet, A. A Continuous Time Framework for Discrete Denoising Models. In *Advances in Neural Information Processing Systems*, October 2022. URL <https://openreview.net/forum?id=DmT862YAieY>.
- Campbell, A., Yim, J., Barzilay, R., Rainforth, T., and Jaakkola, T. Generative Flows on Discrete State-Spaces: Enabling Multimodal Flows with Applications to Protein Co-Design. In *Proceedings of the 41st International Conference on Machine Learning*, pp. 5453–5512. PMLR, July 2024. URL <https://proceedings.mlr.press/v235/campbell124a.html>.
- Chambers, J., Davies, M., Gaulton, A., Hersey, A., Velankar, S., Petryszak, R., Hastings, J., Bellis, L., McGlinchey, S., and Overington, J. P. Unichem: a unified chemical structure cross-referencing and identifier tracking system. *Journal of cheminformatics*, 5(1):3, 2013.
- Chen, R. T., Rubanova, Y., Bettencourt, J., and Duvenaud, D. K. Neural ordinary differential equations. *Advances in neural information processing systems*, 31, 2018.
- Daras, G., Delbraccio, M., Talebi, H., Dimakis, A. G., and Milanfar, P. Soft diffusion: Score matching for general corruptions. *arXiv preprint arXiv:2209.05442*, 2022.
- Dziri, N., Lu, X., Sclar, M., Li, X. L., Jiang, L., Lin, B. Y., Welleck, S., West, P., Bhagavatula, C., Bras, R. L., Hwang, J. D., Sanyal, S., Ren, X., Ettinger, A., Harchaoui, Z., and Choi, Y. Faith and fate: Limits of transformers on compositionality. In *Thirty-seventh Conference on Neural Information Processing Systems*, 2023. URL <https://openreview.net/forum?id=Fkckkr3ya8>.
- Gat, I., Remez, T., Shaul, N., Kreuk, F., Chen, R. T. Q., Synnaeve, G., Adi, Y., and Lipman, Y. Discrete Flow Matching, July 2024. URL <http://arxiv.org/abs/2407.15595>.
- Gillespie, D. T. Approximate accelerated stochastic simulation of chemically reacting systems. *The Journal of chemical physics*, 115(4):1716–1733, 2001.
- Gu, J., Liu, Q., and Cho, K. Insertion-based Decoding with Automatically Inferred Generation Order. *Transactions of the Association for Computational Linguistics*, 7:661–676, 2019. doi: 10.1162/tacl.a.00292. URL <https://aclanthology.org/Q19-1042/>.
- Havasi, M., Karrer, B., Gat, I., and Chen, R. T. Q. Edit Flows: Flow Matching with Edit Operations, June 2025. URL <http://arxiv.org/abs/2506.09018>.
- Ho, J., Jain, A., and Abbeel, P. Denoising diffusion probabilistic models. *Advances in neural information processing systems*, 33:6840–6851, 2020.
- Holderrieth, P., Havasi, M., Yim, J., Shaul, N., Gat, I., Jaakkola, T., Karrer, B., Chen, R. T. Q., and Lipman, Y. Generator matching: Generative modeling with arbitrary markov processes. In *The Thirteenth International Conference on Learning Representations*, 2025. URL <https://openreview.net/forum?id=RuP17cJtZo>.
- Holtzman, A., Buys, J., Du, L., Forbes, M., and Choi, Y. The curious case of neural text degeneration. In *International Conference on Learning Representations*, 2020. URL <https://openreview.net/forum?id=rygGQyrFvH>.

- Hoogeboom, E. and Salimans, T. Blurring diffusion models. *arXiv preprint arXiv:2209.05557*, 2022.
- Hoogeboom, E., Gritsenko, A. A., Bastings, J., Poole, B., van den Berg, R., and Salimans, T. Autoregressive diffusion models, 2022. URL <https://arxiv.org/abs/2110.02037>.
- Huang, P., Liu, T., Liu, Z., Yan, Y., Wang, S., Xiao, T., Chen, Z., and Sun, M. Empirical analysis of decoding biases in masked diffusion models, 2026. URL <https://arxiv.org/abs/2508.13021>.
- Irwin, J. J., Sterling, T., Mysinger, M. M., Bolstad, E. S., and Coleman, R. G. Zinc: a free tool to discover chemistry for biology. *Journal of chemical information and modeling*, 52(7):1757–1768, 2012.
- Kim, J., Cheuk-Kit, L., Domingo-Enrich, C., Du, Y., Kakade, S., Ngotiaoco, T., Chen, S., and Albergo, M. Any-Order Flexible Length Masked Diffusion, September 2025a. URL <http://arxiv.org/abs/2509.01025>.
- Kim, J., Shah, K., Kontonis, V., Kakade, S. M., and Chen, S. Train for the Worst, Plan for the Best: Understanding Token Ordering in Masked Diffusions. In *Forty-Second International Conference on Machine Learning*, June 2025b. URL [https://openreview.net/forum?id=DjJmre5IkP&referrer=%5BReviewers%20Console%5D\(%2Fgroup%3Fid%3DICML.cc%2F2025%2Fconference%2FReviewers%23assigned-submissions\)](https://openreview.net/forum?id=DjJmre5IkP&referrer=%5BReviewers%20Console%5D(%2Fgroup%3Fid%3DICML.cc%2F2025%2Fconference%2FReviewers%23assigned-submissions)).
- Kool, W., van Hoof, H., and Welling, M. Buy 4 REINFORCE samples, get a baseline for free!, 2019. URL <https://openreview.net/forum?id=r1lgTGL5DE>.
- Kumaraswamy, P. A generalized probability density function for double-bounded random processes. *Journal of Hydrology*, 46(1):79–88, 1980. ISSN 0022-1694. doi: 10.1016/0022-1694(80)90036-0. URL <https://www.sciencedirect.com/science/article/pii/0022169480900360>.
- Lee, S., Kreis, K., Veccham, S. P., Liu, M., Reidenbach, D., Peng, Y., Paliwal, S. G., Nie, W., and Vahdat, A. Genmol: A drug discovery generalist with discrete diffusion. In *Forty-second International Conference on Machine Learning*, 2025. URL <https://openreview.net/forum?id=KM7pXWG1xj>.
- Lipman, Y., Chen, R. T., Ben-Hamu, H., Nickel, M., and Le, M. Flow matching for generative modeling. *arXiv preprint arXiv:2210.02747*, 2022.
- Lipman, Y., Havasi, M., Holderrieth, P., Shaul, N., Le, M., Karrer, B., Chen, R. T. Q., Lopez-Paz, D., Ben-Hamu, H., and Gat, I. Flow Matching Guide and Code, December 2024a. URL <http://arxiv.org/abs/2412.06264>.
- Lipman, Y., Havasi, M., Holderrieth, P., Shaul, N., Le, M., Karrer, B., Chen, R. T. Q., Lopez-Paz, D., Ben-Hamu, H., and Gat, I. Flow Matching Guide and Code, December 2024b. URL <http://arxiv.org/abs/2412.06264>. arXiv:2412.06264 [cs].
- Lou, A., Meng, C., and Ermon, S. Discrete diffusion modeling by estimating the ratios of the data distribution. *arXiv preprint arXiv:2310.16834*, 2023.
- Noutahi, E., Gabellini, C., Craig, M., Lim, J. S., and Tossou, P. Gotta be safe: a new framework for molecular design. *Digital Discovery*, 3(4):796–804, 2024.
- Ou, J., Nie, S., Xue, K., Zhu, F., Sun, J., Li, Z., and Li, C. Your absorbing discrete diffusion secretly models the conditional distributions of clean data, 2025. URL <https://arxiv.org/abs/2406.03736>.
- Patel, D., Naseem, T., Pandey, G., Sultan, M. A., McCallum, A., and Astudillo, R. F. Improved sampling from masked diffusion models with position contrastive guidance. In *NeurIPS 2025 Workshop on Structured Probabilistic Inference & Generative Modeling*, 2025a. URL <https://openreview.net/forum?id=e0WmOrWbtc>.
- Patel, D., Sahoo, A., Amballa, A., Naseem, T., Rudner, T. G. J., and McCallum, A. Insertion language models: Sequence generation with arbitrary-position insertions, 2025b. URL <https://arxiv.org/abs/2505.05755>.
- Peebles, W. and Xie, S. Scalable diffusion models with transformers. In *Proceedings of the IEEE/CVF international conference on computer vision*, pp. 4195–4205, 2023.
- Rissanen, S., Heinonen, M., and Solin, A. Generative modelling with inverse heat dissipation. *arXiv preprint arXiv:2206.13397*, 2022.
- Sahoo, S., Arriola, M., Schiff, Y., Gokaslan, A., Marroquin, E., Chiu, J., Rush, A., and Kuleshov, V. Simple and effective masked diffusion language models. *Advances in Neural Information Processing Systems*, 37:130136–130184, 2024a.
- Sahoo, S., Gokaslan, A., De Sa, C. M., and Kuleshov, V. Diffusion models with learned adaptive noise. *Advances in Neural Information Processing Systems*, 37:105730–105779, 2024b.

- Schiff, Y., Sahoo, S. S., Phung, H., Wang, G., Boshar, S., Dalla-torre, H., de Almeida, B. P., Rush, A. M., PIERROT, T., and Kuleshov, V. Simple guidance mechanisms for discrete diffusion models. In *The Thirteenth International Conference on Learning Representations*.
- Shaul, N., Gat, I., Havasi, M., Severo, D., Sriram, A., Holderrith, P., Karrer, B., Lipman, Y., and Chen, R. T. Q. Flow matching with general discrete paths: A kinetic-optimal perspective. In *The Thirteenth International Conference on Learning Representations, 2025*. URL <https://openreview.net/forum?id=tcvMzR2NrP>.
- Shi, J., Han, K., Wang, Z., Doucet, A., and Titsias, M. Simplified and generalized masked diffusion for discrete data. *Advances in neural information processing systems*, 37:103131–103167, 2024.
- Uria, B., Murray, I., and Larochelle, H. A deep and tractable density estimator. In *International Conference on Machine Learning*, 2013. URL <https://api.semanticscholar.org/CorpusID:13147238>.
- Valmeekam, K., Marquez, M., Sreedharan, S., and Kambhampati, S. On the planning abilities of large language models - a critical investigation. In *Thirty-seventh Conference on Neural Information Processing Systems*, 2023. URL <https://openreview.net/forum?id=X6dEqXIsEW>.
- Wang, Z., Shi, J., Heess, N., Gretton, A., and Titsias, M. Learning-Order Autoregressive Models with Application to Molecular Graph Generation. In *Forty-Second International Conference on Machine Learning*, June 2025. URL <https://openreview.net/forum?id=EY6pXIDi3G>.
- Zheng, H., Gong, S., Zhang, R., Chen, T., Gu, J., Zhou, M., Jaitly, N., and Zhang, Y. Continuously Augmented Discrete Diffusion model for Categorical Generative Modeling, October 2025. URL <http://arxiv.org/abs/2510.01329>.

Appendix for Insertion Based Sequence Generation with Learnable Order Dynamics

A	Summary of Notation	12
B	Background: Discrete Flow Matching	14
B.1	Markov Processes on Discrete Spaces	14
B.1.1	Indexed Collections of CTMCs	14
B.2	Discrete Flow Matching	15
C	Projected Discrete Flow Matching	15
C.0.1	Projected rate matching	17
D	Variable length masked diffusion with learnable order dynamics	18
D.1	Target rates (Proof for Proposition 1)	18
D.2	Likelihood under ϕ	21
D.3	Training	22
D.3.1	Projected target rates	22
D.4	Loss function	24
D.5	Gradient computation	25
D.5.1	Full gradient estimator for two parameter sets	26
D.5.2	Schedule regularization	26
D.5.3	Kumaraswamy schedules	27
D.5.4	Probability of an order under Kumaraswamy Schedule	28
D.6	Sampling	28
D.7	Truncation vs Rescaling	30
E	Details of the experiment setup	30
E.1	Graph Traversal	30
E.2	Molecule Generation	31
F	Additional Results and Analyses	31
F.1	Flexibility vs Stability	31
F.2	Star Graph Traversal	31
F.2.1	Examples: Generation Order	31
G	Related Work	34

A. Summary of Notation

Table 3 summarizes the notation used throughout the paper.

Notation	Description
General	
\mathbb{X}, \mathbb{Z}	Sets (blackboard font)
$\llbracket n \rrbracket$	Set of natural numbers $\{1, 2, \dots, n\}$
x_t	Particular state at time t of a stochastic process X_t
x_t^i, s^i, w^i , etc.	i -th component of x, s, w respectively, i.e. superscript i denotes the i -th component in a sequence
$\delta_x(y) = \delta_{\{x\}}(y)$	Indicator function that is 1 if $x = y$ and 0 otherwise
$p_t(x)$	The marginal law of CTMC X_t at time t , i.e., $p_t(x) = \mathbb{P}(X_t = x)$
$p_{t s}(x y)$	The conditional law of CTMC X_t at time t given the value at time s , i.e., $p_{t s}(x y) = \mathbb{P}(X_t = x X_s = y)$
$p_{t C}(x c)$	The conditional law of CTMC X_t at time t given the conditioning variable $C = c$, i.e., $p_{t C}(x c) = \mathbb{P}(X_t = x C = c)$
$R_t(x, y)$	The rate of the transition from x to y at time t , i.e., $R_t(x, y) = \lim_{h \rightarrow 0} \frac{\mathbb{P}(X_{t+h}=y X_t=x) - \delta_x(y)}{h}$
$R_t(x, y c)$	The conditional rate of the transition from x to y at time t given the conditioning variable $C = c$. $R_t(x, y c)$ generates $p_{t C}(x c)$ in the sense of Definition 1.
Specific variables	
$\llbracket \text{D} \rrbracket$	Drop token
$\llbracket \text{M} \rrbracket$	Mask token
\mathbb{V}	Vocabulary of tokens including the $\llbracket \text{M} \rrbracket$ token but excluding the $\llbracket \text{D} \rrbracket$ token
\mathbb{V}^n	Set of token sequences of length n , i.e., $\mathbb{V}^n = \mathbb{V} \times \dots \times \mathbb{V}$ (n times)
\mathbb{X}	Space of variable length sequences, i.e., $\mathbb{X} = \bigcup_{k=1}^L \mathbb{V}^k$
\mathbb{Z}	Auxiliary space of partial sequences, i.e., $\mathbb{Z} = \bigcup_{k \in \llbracket L \rrbracket} \mathbb{V}^k \times \mathbb{S}_k$, where $\mathbb{S}_k := \{(s^1, \dots, s^k) \in \llbracket L \rrbracket^k \mid s^1 < \dots < s^k\}$ is the space of ordered tuples of positions
$\bar{\mathbb{Z}}$	Auxiliary space of partial sequences with the $\llbracket \text{D} \rrbracket$ token added to the vocabulary, i.e., $\bar{\mathbb{Z}} = (\mathbb{V} \cup \{\llbracket \text{D} \rrbracket\})^L$, with isomorphism $f_{\text{contract}} : \bar{\mathbb{Z}} \rightarrow \mathbb{Z}$ that removes the $\llbracket \text{D} \rrbracket$ tokens from the \bar{z} to form x , and moves the exact position information to s to produce $z = (x, s)$
$R_t^i(z, w^i \mid (z_1, z_0))$	The per-position target rate of the transition from z to w^i at time t given the conditioning variable (z_1, z_0) , i.e., $R_t^i(z, w^i \mid (z_1, z_0)) = \lambda_t^i(z; (z_1, z_0)) \cdot K_t^i(z, w^i \mid (z_1, z_0))$
$\lambda_t^i(z; (z_1, z_0))$	The state and time dependent arrival rate of the Poisson process at the i -th position at time t given the conditioning variable (z_1, z_0)
$K_t^i(z, w^i \mid (z_1, z_0))$	The state transition kernel at the i -th position at time t given the conditioning variable (z_1, z_0) , i.e., when an arrival occurs at the i -th position, the state changes according to the categorical distribution K_t^i
$T_{\text{in}}^i := T_1^i$	The event time of the insertion event at the i -th position
$T_{\text{um}}^i := T_2^i$	The event time of the unmasking event at the i -th position

Table 3. Summary of notation used throughout the paper.

B. Background: Discrete Flow Matching

B.1. Markov Processes on Discrete Spaces

Let \mathbb{X} be countable set (e.g. the vocabulary \mathbb{V} or the space of sequences of length L with tokens from \mathbb{V}), and $\{X_t\}$ be a continuous time stochastic process on \mathbb{X} .

$$p_{t+h|t}(x_{t+h}|x_t) := \mathbb{P}(X_{t+h} = x_{t+h}|X_t = x_t) = \delta_{x_t}(x_{t+h}) + h R_t(x_t, x_{t+h}) + o(h), \quad (13)$$

where $R_t(x, y)$ is the *rate* of the transition from x to y at time t , such that $R_t(x, x) = -\sum_{y \neq x} R_t(x, y)$. Equivalently, $R_t(x, y) = \lim_{h \rightarrow 0} \frac{\mathbb{P}(X_{t+h}=y|X_t=x) - \delta_x(y)}{h}$.

The Kolmogorov Forward Equation (KFE) is the central continuity equation for CTMCs. It connects the marginal probabilities to the rate:

$$\partial_t p_t(x) = \sum_y R_t(y, x) p_t(y). \quad (14)$$

Definition 1 (Time marginals generated by CTMC). We note that the following statements are equivalent (Campbell et al., 2024):

- $R_t(\cdot, \cdot)$ **generates** p_t
- $R_t(\cdot, \cdot)$ and p_t satisfy the KFE in the marginal form (Equation (14))
- A Markov process X_t with rates $R_t(\cdot, \cdot)$ and initial distribution p_0 has p_t as its marginal distribution at time t

B.1.1. INDEXED COLLECTIONS OF CTMCs

Definition 2 (Conditional Rates). For a general variable $C \in \mathcal{C}$ with distribution π ,

- denote C dependent rates as $R_t(x, y|C)$
- denote by $\{\{X_t^c\}\}_{c \in \mathcal{C}}$ a collection of CTMCs on \mathbb{X} with rates $R_t(x, y|C)$ and initial distribution $p_0(x|C)$
- $p_{t|C}(x|c) := \mathbb{P}(X_t^c = x)$ denote the marginals of the CTMC $\{X_t^c\}$

In the special case of endpoint indexed collection, we have $C = (X_0, X_1)$, $X_1 \sim p_{\text{data}}$ and $X_0 \sim \pi(x_0|x_1)$, where π is the coupling distribution (Gat et al., 2024).

Proposition 2 (Mixture of CTMCs). *The mixture rate $R_t(x, \cdot) = \mathbb{E}_{C|X_t=x}[R_t(x, \cdot|C)]$ generates the marginals $p_t(x) = \mathbb{E}_C[p_{t|C}(x|C)]$.*

The proof assumes mild regularity conditions and follows from a straightforward application of the KFE (see Campbell et al. (2024) or Lipman et al. (2024b) Thm. 14 for details). This result shows there exists a rate matrix $R_t(\cdot, \cdot) = \mathbb{E}_C[R_t(\cdot, \cdot|C)]$ and the corresponding CTMC $\{X_t\}$ such that R_t generates $p_t(x) = \mathbb{E}_C[p_{t|C}(x|C)]$. Therefore, in order to sample from the data distribution p_1 , we can follow:

1. Pick the indexing set $C = (X_0, X_1)$
2. Use $p_1 = p_{\text{data}}$ and pick the coupling distribution $\pi(x_0|x_1)$, typically independent i.e. $\pi(x_0|x_1) = p_0(x_0)$ for some easy to sample p_0 .
3. Construct a collection of CTMCs $\{X_t^c\}_{c \in \mathcal{C}}$ with rates $R_t(x, y|C)$ such that it generates $p_{t|C}$, which satisfies $p_{1|C}(x|x_1, x_0) = \delta_{x_1}(x)$ and $p_{0|C}(x|x_0, x_0) = \delta_{x_0}(x)$.
4. The marginal $p_t(x) = \mathbb{E}_C[p_{t|C}(x|C)]$ satisfies $p_1(x) = p_{\text{data}}(x)$ and Proposition 2 ensures that the CTMC with the rate $R_t(\cdot, \cdot) = \mathbb{E}_C[R_t(\cdot, \cdot|C)]$ generates the marginals $p_t(x) = \mathbb{E}_C[p_{t|C}(x|C)]$.
5. Construct an optimization problem to learn parametric $R_t^\theta(\cdot, \cdot)$.

Next we look at the optimization objective for learning the rates R_t .

B.2. Discrete Flow Matching

We want to learn the rates $R_t(x, y)$ using a parametric model $R_t^\theta(x, y)$. Since we can easily write down the conditional rates $R_t(x, y|z)$ we can use appropriate loss function to match $R_t^\theta(x, \cdot)$ with $R_t(x, \cdot) = \mathbb{E}_{z \sim p_{Z|t}(\cdot|x)} R_t(x, \cdot|z)$. That is for some distance measure D , we want to minimize:

$$\mathcal{L}(\theta) = \mathbb{E}_{X_t \sim p_t} D\left(\mathbb{E}_{C \sim p_{C|t}(\cdot|X_t)} R_t(X_t, \cdot|C), R_t^\theta(X_t, \cdot)\right),$$

where the expectations are over $x_t \sim p_t$ and $C \sim \pi(\cdot|x_t)$.

In most cases, this objective is not useful in this form, but for Bregman divergence, we have [Holderrieth et al. \(2025\)](#) convexity in the first argument and linearity of the gradient w.r.t convex combinations in the first argument. Recall the definition of Bregman divergence $D_F(b, a)$ defined for any convex function F is given by:

$$D_F(b, a) = F(b) - F(a) - \nabla F(a) \cdot (b - a), \quad (15)$$

where $\nabla F(a)$ is the gradient of F at a .

Convexity in the first argument It is convex in the first argument. Meaning that $\lambda D_F(b_1, a) + (1 - \lambda) D_F(b_2, a) \geq D_F(\lambda b_1 + (1 - \lambda)b_2, a)$ for all $\lambda \in [0, 1]$. This is easy to see:

$$\begin{aligned} D_F(\lambda b_1 + (1 - \lambda)b_2, a) &= F(\lambda b_1 + (1 - \lambda)b_2) - F(a) - \nabla F(a) \cdot (\lambda b_1 + (1 - \lambda)b_2 - a) \\ &\leq \lambda F(b_1) + (1 - \lambda)F(b_2) - F(a) - \nabla F(a) \cdot (\lambda b_1 + (1 - \lambda)b_2 - a) \\ &= \lambda[F(b_1) - F(a) - \nabla F(a) \cdot (b_1 - a)] \\ &\quad + (1 - \lambda)[F(b_2) - F(a) - \nabla F(a) \cdot (b_2 - a)] \\ &= \lambda D_F(b_1, a) + (1 - \lambda) D_F(b_2, a) \end{aligned} \quad (16)$$

Gradient is linear for convex combinations in the first argument. Its gradient with respect to the second argument is **linear** w.r.t affine combinations in the first argument ([Holderrieth et al., 2025](#)). This is a consequence of the expression for the gradient w.r.t the second argument, which is given by

$$\nabla_a D_F(b, a) = -\nabla^2 F(a)(b - a), \quad (17)$$

where $\nabla^2 F(a)$ is the Hessian of F at a . Clearly, $f(b) = \nabla_a D_F(b, a)$ is linear in b . Therefore, under convex combinations, which can be extended to expectations, we get:

$$\begin{aligned} \nabla_a D_F(\lambda b_1 + (1 - \lambda)b_2, a) &= \lambda \nabla_a D_F(b_1, a) + (1 - \lambda) \nabla_a D_F(b_2, a) \\ \nabla_a [D_F(\mathbb{E} Y, a)] &= \mathbb{E}[\nabla_a D_F(Y, a)]. \end{aligned} \quad (18)$$

Therefore for $C = X_1$ we can use the following objective to train the parameters of $R_t^\theta(x, y)$:

$$\mathcal{L}(\theta) = \mathbb{E}_{X_1 \sim p_{\text{data}}, X_0 \sim p_{t|X_1}} [D_F(R_t(X, \cdot|X_1), R_t^\theta(X, \cdot))]. \quad (19)$$

C. Projected Discrete Flow Matching

In this section, we will discuss a type of *weak* intertwining of two Markov processes that depends on the law of the main process. This is a generalization of the flow matching with auxiliary variables ([Havasi et al., 2025](#)) and the joint interpolants ([Kim et al., 2025a](#)), in that we allow probabilistic mappings between the two spaces.

Let \mathbb{X} and \mathbb{Z} be two countable state spaces, and let $\pi_{\text{enc}}(x|z)$ be probability kernel from \mathbb{Z} to \mathbb{X} .

Definition 3. Let $\{Z_t\}$ be a CTMC on \mathbb{Z} with rate matrix R_t and initial distribution $p_0(z)$. Then the CTMC $\{X_t\}$ on \mathbb{X} with rate matrix R_t^π is said to be a *weakly intertwined projection* of Z_t under the encoder π_{enc} if

$$R_t^\pi(x, y) = \sum_{z \in \mathbb{Z}} \sum_{w \in \mathbb{Z}} \pi_{\text{enc}}(y|w) \pi_{\text{dec}, t}(z|x) R_t(z, w), \quad (20)$$

where $\pi_{\text{dec},t}(z|x)$ is the time and law dependent Bayes' decoder given by:

$$\pi_{\text{dec},t}(z|x) = \frac{p_t(z)\pi_{\text{enc}}(x|z)}{p_t(x)}, \quad p_t(x) > 0, \quad (21)$$

where $p_t(x) := \mathbb{P}(X_t = x)$ and $p_t(z) := \mathbb{P}(Z_t = z)$ are the marginal laws of $\{X_t\}$ and $\{Z_t\}$ respectively.

Proposition 3 (R_t^π generates $p_t(x)$). *Let $\{X_t\}$ be a weakly intertwined projection of $\{Z_t\}$ under the encoder π_{enc} . Then R_t^π as defined in Equation (20) generates $p_t(x)$ in the sense of Definition 1.*

Proof. We can easily see that R_t^π generates $p_t(x) = \mathbb{E}_{z \sim p_t}[\pi_{\text{enc}}(x|z)]$ by checking the KFE:

$$\begin{aligned} \partial_t p_t(x) &= \partial_t \sum_{z \in \mathbb{Z}} p_t(z) \pi_{\text{enc}}(x|z) \\ &= \sum_{z \in \mathbb{Z}} \partial_t p_t(z) \pi_{\text{enc}}(x|z) \\ &= \sum_{z \in \mathbb{Z}} \left[\sum_{w \in \mathbb{Z}} p_t(w) R_t(w, z) \right] \pi_{\text{enc}}(x|z) \\ &= \sum_{z \in \mathbb{Z}} \left[\sum_{w \in \mathbb{Z}} \sum_{y \in \mathbb{X}} \pi_{\text{dec},t}(w|y) p_t(y) R_t(w, z) \right] \pi_{\text{enc}}(x|z) \quad (\text{by Equation (21)}) \\ &= \sum_{y \in \mathbb{X}} R_t^\pi(y, x) p_t(y) \quad (\text{by Equation (20)}) \end{aligned} \quad (22)$$

□

Similarly, for any conditioning variable C , we can define the C dependent rates analogous to Definition 2 as:

$$R_t^\pi(x, y|C) = \sum_{z \in \mathbb{Z}} \sum_{w \in \mathbb{Z}} \pi_{\text{enc}}(y|w) \pi_{\text{dec},t}(z|x, C) R_t(z, w|C), \quad (23)$$

where the Bayes decoder is given by:

$$\pi_{\text{dec},t}(z|x, C) = \frac{p_{t|C}(z|C) \pi_{\text{enc}}(x|z)}{p_{t|C}(x|C)}, \quad p_{t|C}(x|C) > 0. \quad (24)$$

We can show that with $p_{t|C}(x|C) := \sum_{z \in \mathbb{Z}} p_{t|C}(z|C) \pi_{\text{enc}}(x|z)$,

$$\partial_t p_{t|C}(x|C) = \sum_y R_t^\pi(y, x|C) p_{t|C}(y|C). \quad (25)$$

That is, $R_t^\pi(x, y|C)$ generates $p_{t|C}(x|C)$:

$$\begin{aligned} \partial_t p_{t|C}(x|C) &= \partial_t \sum_{z \in \mathbb{Z}} p_{t|C}(z|C) \pi_{\text{enc}}(x|z) \\ &= \sum_{z \in \mathbb{Z}} \partial_t p_{t|C}(z|C) \pi_{\text{enc}}(x|z) \\ &= \sum_{z \in \mathbb{Z}} \left[\sum_{w \in \mathbb{Z}} p_{t|C}(w|C) R_t(w, z|C) \right] \pi_{\text{enc}}(x|z) \\ &= \sum_{z \in \mathbb{Z}} \left[\sum_{w \in \mathbb{Z}} \sum_{y \in \mathbb{X}} \pi_{\text{dec},t}(w|y, C) p_{t|C}(y|C) R_t(w, z|C) \right] \pi_{\text{enc}}(x|z) \quad (\text{by Equation (24)}) \\ &= \sum_{y \in \mathbb{X}} R_t^\pi(y, x|C) p_{t|C}(y|C) \quad (\text{by Equation (23)}) \end{aligned} \quad (26)$$

Remark 3 (Degenerate (Dirac) decoders preserve the KFE). The Bayes decoder $\pi_{\text{dec},t}(z|x, C)$ in Equation (23) averages over all latent states z compatible with the observed state x (and condition C). As we will see later that we can additionally condition on *side information* H (e.g., an alignment/position tuple) such that the latent state can be selected deterministically from (x, H) . In this case we can use a degenerate decoder

$$\pi_{\text{dec},t}(z|x, C, H) = \delta_z(\varphi(x, H)). \quad (27)$$

Defining projected rates using Equation (23) with the enlarged condition (C, H) , the same calculation as above shows that the KFE remains satisfied:

$$\partial_t p_{t|C,H}(x|C, H) = \sum_y R_t^\pi(y, x|C, H) p_{t|C,H}(y|C, H). \quad (28)$$

If desired, one can marginalize out H via the mixture identity $R_t^\pi(x, y|C) = \mathbb{E}_{H \sim p_{H|t}(\cdot|x, C)}[R_t^\pi(x, y|C, H)]$.

Following is the key result stating that the projected rates generate the desired time marginals just like vanilla DFM without auxiliary variables.

Proposition 4 (R_t^π generates p_t). *Let $\{X_t\}$ be a weakly intertwined projection of $\{Z_t\}$ under the encoder π_{enc} . Then R_t^π as defined in Equation (20) generates p_t in the sense of Definition 1.*

Proof. We show that $R_t^\pi(x, y) := \mathbb{E}_{C \sim p_{C|t}(\cdot|x)}$ $R_t^\pi(x, y|C)$ generates $p_t(x) = \mathbb{E}_C p_{t|C}(x|C)$ by checking the KFE. (In particular, this argument applies verbatim if we enlarge the conditioning variable from C to (C, H) to incorporate auxiliary side information H .)

$$\begin{aligned} \partial_t p_t(x) &= \sum_C p(C) \partial_t p_{t|C}(x|C) \\ &= \sum_C p(C) \sum_y R_t^\pi(y, x|C) p_{t|C}(y|C) \quad (\text{by Equation (25)}) \\ &= \sum_y \sum_C R_t^\pi(y, x|C) p_{C|t}(C|y) p_t(y) \\ &= \sum_y R_t^\pi(y, x) p_t(y). \end{aligned} \quad (29)$$

□

Proposition 4 provides us a way to construct the desired probability path on \mathbb{X} that satisfies the boundary conditions $p_0 = p$ and $p_1 = p_{\text{data}}$, by constructing conditional rates $R_t(z, w|C)$ in the auxiliary space \mathbb{Z} and selecting appropriate encoder π_{enc} to obtain $R_t^\pi(x, y|C)$. This approach comes in handy when it is easier to construct probability path on the auxiliary space \mathbb{Z} than the original space \mathbb{X} .

C.0.1. PROJECTED RATE MATCHING

Even though the probability paths are constructed in the auxiliary space, we still want to learn the rates in the original space \mathbb{X} .

$$\mathbb{E}_{X_t, C} D_F(R_t^\pi(X_t, \cdot|C), R_t^\theta(X_t, \cdot))$$

The question, however, is whether this is the same as

$$\mathbb{E}_{X_t} D_F(R_t^\pi(X_t, \cdot), R_t^\theta(X_t, \cdot)).$$

Due to the convexity in the first argument of Bregman divergence, we see that the two expressions are not equal in general: the first one is an upper bound for the second one.

Recall from earlier that $R_t^\pi(x, y) = \mathbb{E}_{C \sim p_{C|t}(\cdot|x)} R_t^\pi(x, y|C)$. Using this, we can rewrite the second expression as:

$$\mathbb{E}_{X_t} D_F(R_t^\pi(X_t, \cdot), R_t^\theta(X_t, \cdot)) = \mathbb{E}_{X_t} D_F \left(\mathbb{E}_{C|X_t} R_t^\pi(X_t, \cdot|C), R_t^\theta(X_t, \cdot) \right).$$

Since $D_F(b, a)$ is convex in the first argument b , by Jensen's inequality we have:

$$D_F \left(\mathbb{E}_{C|X_t} R_t^\pi(X_t, \cdot|C), R_t^\theta(X_t, \cdot) \right) \leq \mathbb{E}_{C|X_t} [D_F(R_t^\pi(X_t, \cdot|C), R_t^\theta(X_t, \cdot))].$$

Taking expectations over X_t on both sides:

$$\begin{aligned} \mathbb{E}_{X_t} D_F \left(\mathbb{E}_{C|X_t} R_t^\pi(X_t, \cdot|C), R_t^\theta(X_t, \cdot) \right) &\leq \mathbb{E}_{X_t} \left[\mathbb{E}_{C|X_t} D_F(R_t^\pi(X_t, \cdot|C), R_t^\theta(X_t, \cdot)) \right] \\ &= \mathbb{E}_{X_t, C} D_F(R_t^\pi(X_t, \cdot|C), R_t^\theta(X_t, \cdot)). \end{aligned}$$

Therefore:

$$\mathbb{E}_{X_t} D_F(R_t^\pi(X_t, \cdot), R_t^\theta(X_t, \cdot)) \leq \mathbb{E}_{X_t, C} D_F(R_t^\pi(X_t, \cdot|C), R_t^\theta(X_t, \cdot)). \quad (30)$$

Proposition 5 (Projected rate matching upper bounds terminal KL). *Let $\{X_t\}_{t \in [0,1]}$ be a time-inhomogeneous CTMC on \mathbb{X} with initial distribution p_0 and (marginal) projected rates $R_t^\pi(\cdot, \cdot)$. Let $\{\hat{X}_t\}$ be another CTMC on \mathbb{X} with the same initial distribution p_0 and model rates $R_t^\theta(\cdot, \cdot)$. Assume absolute continuity of the jump intensities: for all $t \in [0, 1]$ and $x \neq y$, $R_t^\pi(x, y) > 0$ implies $R_t^\theta(x, y) > 0$, and assume the expectations below are finite.*

Let \mathbb{P}^π and \mathbb{P}^θ denote the corresponding path measures on $[0, 1]$, and let p_1^π and p_1^θ be the terminal marginals of X_1 and \hat{X}_1 . Define D_F to be the Bregman divergence generated by $F(a) = \sum_{y \neq x} a_y \log a_y$ applied to the off-diagonal rate vectors $R_t(x, \cdot) := (R_t(x, y))_{y \neq x}$. Then:

$$\mathcal{D}_{\text{KL}}(p_1^\pi \| p_1^\theta) \leq \mathcal{D}_{\text{KL}}(\mathbb{P}^\pi \| \mathbb{P}^\theta) = \int_0^1 \mathbb{E}_{\mathbb{P}^\pi} [D_F(R_t^\pi(X_t, \cdot), R_t^\theta(X_t, \cdot))] dt. \quad (31)$$

Moreover, if the projected rates arise as a conditional mixture $R_t^\pi(x, \cdot) = \mathbb{E}_{C \sim p_{C|t}(\cdot|x)} [R_t^\pi(x, \cdot|C)]$, then for every t ,

$$\mathbb{E}_{\mathbb{P}^\pi} [D_F(R_t^\pi(X_t, \cdot), R_t^\theta(X_t, \cdot))] \leq \mathbb{E}_{(X_t, C)} [D_F(R_t^\pi(X_t, \cdot|C), R_t^\theta(X_t, \cdot))], \quad (32)$$

where $C \sim p_{C|t}(\cdot|X_t)$ in the right-hand side. Consequently,

$$\mathcal{D}_{\text{KL}}(p_1^\pi \| p_1^\theta) \leq \int_0^1 \mathbb{E}_{(X_t, C)} [D_F(R_t^\pi(X_t, \cdot|C), R_t^\theta(X_t, \cdot))] dt. \quad (33)$$

Proof. The inequality $\mathcal{D}_{\text{KL}}(p_1^\pi \| p_1^\theta) \leq \mathcal{D}_{\text{KL}}(\mathbb{P}^\pi \| \mathbb{P}^\theta)$ follows by data processing inequality, since X_1 is a measurable function of the full path. The path-space identity is the standard Radon–Nikodym derivative formula for time-inhomogeneous CTMCs, which yields $\mathcal{D}_{\text{KL}}(\mathbb{P}^\pi \| \mathbb{P}^\theta) = \int_0^1 \mathbb{E}_{\mathbb{P}^\pi} [D_F(R_t^\pi(X_t, \cdot), R_t^\theta(X_t, \cdot))] dt$ when $F(a) = \sum a \log a$ is applied to the off-diagonal jump intensities. Finally, the conditional-mixture upper bound is exactly Equation (30) applied pointwise in t , and integrating over t gives the final inequality. For a simple proof using discretization arguments, see [Shaul et al. \(2025\)](#). \square

D. Variable length masked diffusion with learnable order dynamics

D.1. Target rates (Proof for Proposition 1)

In order to construct the target probability paths, we will set $h = (z_0, z_1)$, where $z_1 \sim p_1(z_1)$, where $p_1(z_1)$ is the distribution over $\bar{\mathbb{Z}}$ obtained by padding the ground truth sequences $x_1 \sim p_{\text{data}}(x_1)$ with [D] tokens to length L , and $z_0 \sim p_0(z_0)$, where $p_0(z_0)$ places all mass on the sequence of length L with all [D] tokens.

Now we have two times T_{in} and T_{um} that need to be sampled ensuring that $T_{\text{in}} < T_{\text{um}}$, i.e., insertion happens before unmasking.

Notation: In the following, the CDFs $F_{\text{in}}^{\phi,i}(t; z_1)$ and $F_{\text{um}}^{\phi,i}(t; z_1)$ depend on the learnable parameters ϕ and the target sequence z_1 ; for brevity we suppress this dependence in the notation and write $F_{\text{in}}^i(t)$ and $F_{\text{um}}^i(t)$ throughout this proof.

We first choose an insertion time distribution by specifying its CDF:

$$\mathbb{P}(T_{\text{in}}^i \leq t) = F_{\text{in}}^i(t), \quad f_{T_{\text{in}}^i}(t) = \frac{d}{dt} F_{\text{in}}^i(t). \quad (34)$$

such that $F_{\text{in}}^i(0) = 0$ and $F_{\text{in}}^i(1) = 1$. We then define the conditional distribution of T_{um}^i given $T_{\text{in}}^i = s$ by **truncating** a base distribution of a random variable U^i on $[0, 1]$ to $[s, 1]$. Let the base distribution have CDF $F_{\text{um}}^i(u)$, again such that $F_{\text{um}}^i(0) = 0$ and $F_{\text{um}}^i(1) = 1$. Throughout this proof, we use the density notation $f_{T_{\text{in}}^i}(t) \equiv \dot{F}_{\text{in}}^i(t)$ and $f_{U^i}(t) \equiv \dot{F}_{\text{um}}^i(t)$ (or equivalently $\frac{d}{dt} F_{*}^i(t)$), consistent with the proposition's dot notation. Then

$$\mathbb{P}(T_{\text{um}}^i \leq t \mid T_{\text{in}}^i = s) = \delta(t \geq s) \left[\frac{\mathbb{P}(U^i \leq t) - \mathbb{P}(U^i \leq s)}{1 - \mathbb{P}(U^i \leq s)} \right], \quad (35)$$

$$f_{T_{\text{um}}^i | T_{\text{in}}^i = s}(t) = \delta(t \geq s) \frac{f_{U^i}(t)}{\mathbb{P}(U^i > s)} = \delta(t \geq s) \frac{\dot{F}_{\text{um}}^i(t)}{1 - F_{\text{um}}^i(s)} \quad (36)$$

for $t \in [0, 1]$. This construction guarantees $T_{\text{in}}^i < T_{\text{um}}^i$ almost surely.

Conditional probability paths: Viewing z and z_1 as elements of $\bar{\mathbb{Z}}$, per-token conditional probability paths in the augmented space $\bar{\mathbb{Z}}$ are given by:

$$\begin{aligned} p_t^{\phi,i}(z^i | z_1, z_0) &= \underbrace{\mathbb{P}(T_{\text{in}}^i > t) \delta_{[\text{D}]}(z^i)}_{p_t^{\phi,i}([\text{D}] | z_1, z_0)} \\ &\quad + \underbrace{\mathbb{P}(T_{\text{in}}^i \leq t < T_{\text{um}}^i) \delta_{[\text{M}]}(z^i) (1 - \delta_{z_1^i}([\text{D}]))}_{p_t^{\phi,i}([\text{M}] | z_1, z_0)} \\ &\quad + \underbrace{\mathbb{P}(T_{\text{um}}^i \leq t) \delta_{z_1^i}(z^i)}_{p_t^{\phi,i}(z_1^i | z_1, z_0)}, \end{aligned} \quad (37)$$

where $T_{\text{in}}, T_{\text{um}}$ depend on z_1 and ϕ through Equations (34) and (35), and $z_0 = [\text{D}]$ always. Note the additional indicator function $(1 - \delta_{z_1^i}([\text{D}]))$ ensures that if $z_1^i = [\text{D}]$ (i.e. a pad to the right of the clean sequence), then no change happens.

Target conditional rates Fix a token position i and assume $z_1^i \neq [\text{D}]$ (otherwise the process stays at $[\text{D}]$ and all rates are 0). At this position, the process has three states $\{[\text{D}], [\text{M}], z_1^i\}$ with transitions

$$[\text{D}] \xrightarrow{T_{\text{in}}^i} [\text{M}] \xrightarrow{T_{\text{um}}^i} z_1^i,$$

where the first jump happens at time T_{in}^i and the second at time T_{um}^i . We will take the time derivative of Equation (37) to obtain the LHS of the KFE Equation (14). Going term by term, we have the following

Derivative 1:

$$\partial_t \mathbb{P}(T_{\text{in}}^i > t) = \partial_t (1 - F_{\text{in}}^i(t)) = -f_{T_{\text{in}}^i}(t) \quad (38)$$

$$= -\frac{f_{T_{\text{in}}^i}(t)}{\mathbb{P}(T_{\text{in}}^i > t)} \mathbb{P}(T_{\text{in}}^i > t) \quad (39)$$

$$:= -\lambda_{\text{in}}^i(t) \mathbb{P}(T_{\text{in}}^i > t) \quad (40)$$

Derivative 2: Due to the partition $\{T_{\text{in}}^i \leq t\} = \{T_{\text{in}}^i \leq t < T_{\text{um}}^i\} \sqcup \{T_{\text{um}}^i \leq t\}$, we have

$$\partial_t \mathbb{P}(T_{\text{in}}^i \leq t < T_{\text{um}}^i) = \partial_t \mathbb{P}(T_{\text{in}}^i \leq t) - \partial_t \mathbb{P}(T_{\text{um}}^i \leq t) \quad (41)$$

$$= -\partial_t \mathbb{P}(T_{\text{in}}^i > t) - \partial_t \mathbb{P}(T_{\text{um}}^i \leq t) \quad (42)$$

$$= \lambda_{\text{in}}^i(t) \mathbb{P}(T_{\text{in}}^i > t) - f_{T_{\text{um}}^i}(t) \quad (43)$$

Derivative 3:

$$\partial_t \mathbb{P}(T_{\text{um}}^i \leq t) = \frac{d}{dt} \int_0^t \mathbb{P}(T_{\text{um}}^i \leq t \mid T_{\text{in}}^i = s) f_{T_{\text{in}}^i}(s) ds \quad (44)$$

$$= \mathbb{P}(T_{\text{um}}^i \leq t \mid T_{\text{in}}^i = t) f_{T_{\text{in}}^i}(t) + \int_0^t \frac{\partial}{\partial t} \mathbb{P}(T_{\text{um}}^i \leq t \mid T_{\text{in}}^i = s) f_{T_{\text{in}}^i}(s) ds \quad (45)$$

$$= 0 \cdot f_{T_{\text{in}}^i}(t) + \int_0^t f_{T_{\text{um}}^i \mid T_{\text{in}}^i = s}(t) f_{T_{\text{in}}^i}(s) ds \quad (46)$$

$$= f_{T_{\text{um}}^i}(t) \quad (47)$$

$$= \frac{f_{T_{\text{um}}^i}(t)}{\mathbb{P}(T_{\text{in}}^i \leq t < T_{\text{um}}^i)} \mathbb{P}(T_{\text{in}}^i \leq t < T_{\text{um}}^i) \quad (48)$$

$$:= \lambda_{\text{um}}^i(t) \mathbb{P}(T_{\text{in}}^i \leq t < T_{\text{um}}^i) \quad (49)$$

where we define the unmasking rate as

$$\lambda_{\text{um}}^i(t) := \frac{f_{T_{\text{um}}^i}(t)}{\mathbb{P}(T_{\text{in}}^i \leq t < T_{\text{um}}^i)}. \quad (50)$$

Substituting back into Derivative 2:

$$\partial_t \mathbb{P}(T_{\text{in}}^i \leq t < T_{\text{um}}^i) = \lambda_{\text{in}}^i(t) \mathbb{P}(T_{\text{in}}^i > t) - \lambda_{\text{um}}^i(t) \mathbb{P}(T_{\text{in}}^i \leq t < T_{\text{um}}^i) \quad (51)$$

Putting all three derivatives together, from Equation (37) we have:

$$\partial_t p_t^{\phi, i}(z^i \mid z_1, z_0) = -\lambda_{\text{in}}^i(t) \mathbb{P}(T_{\text{in}}^i > t) \delta_{[\text{D}]}(z^i) \quad (52)$$

$$+ [\lambda_{\text{in}}^i(t) \mathbb{P}(T_{\text{in}}^i > t) - \lambda_{\text{um}}^i(t) \mathbb{P}(T_{\text{in}}^i \leq t < T_{\text{um}}^i)] \delta_{[\text{M}]}(z^i) \cdot \bar{\delta}_{z_1^i}([\text{D}]) \quad (53)$$

$$+ \lambda_{\text{um}}^i(t) \mathbb{P}(T_{\text{in}}^i \leq t < T_{\text{um}}^i) \delta_{z_1^i}(z^i) \quad (54)$$

$$= \lambda_{\text{in}}^i(t) \mathbb{P}(T_{\text{in}}^i > t) [\delta_{[\text{M}]}(z^i) \bar{\delta}_{z_1^i}([\text{D}]) - \delta_{[\text{D}]}(z^i)] \quad (55)$$

$$+ \lambda_{\text{um}}^i(t) \mathbb{P}(T_{\text{in}}^i \leq t < T_{\text{um}}^i) [\delta_{z_1^i}(z^i) - \delta_{[\text{M}]}(z^i) \bar{\delta}_{z_1^i}([\text{D}])] \quad (56)$$

For the sake of compactness, from here on, we will not write $\bar{\delta}_{z_1^i}([\text{D}])$ explicitly, as it is only present to handle the case of $z_1^i = [\text{D}]$.

$$\partial_t p_t^{\phi, i}(z^i \mid z_1, z_0) = \lambda_{\text{in}}^i(t) p_t^{\phi, i}([\text{D}] \mid z_1, z_0) [\delta_{[\text{M}]}(z^i) - \delta_{[\text{D}]}(z^i)] \quad (57)$$

$$+ \lambda_{\text{um}}^i(t) p_t^{\phi, i}([\text{M}] \mid z_1, z_0) [\delta_{z_1^i}(z^i) - \delta_{[\text{M}]}(z^i)]$$

$$= \sum_{y^i \in \{[\text{D}], [\text{M}], z_1^i\}} [\lambda_{\text{in}}^i(t) (\delta_{[\text{M}]}(z^i) - \delta_{y^i}(z^i)) \delta_{[\text{D}]}(y^i)$$

$$+ \lambda_{\text{um}}^i(t) (\delta_{z_1^i}(z^i) - \delta_{y^i}(z^i)) \delta_{[\text{M}]}(y^i)] p_t^{\phi, i}(y^i \mid z_1, z_0)$$

$$= \sum_{y^i \in \mathbb{V} \cup \{[\text{D}], [\text{M}]\}} [\lambda_{\text{in}}^i(t) (\delta_{[\text{M}]}(z^i) - \delta_{y^i}(z^i)) \delta_{[\text{D}]}(y^i)$$

$$+ \lambda_{\text{um}}^i(t) (\delta_{z_1^i}(z^i) - \delta_{y^i}(z^i)) \delta_{[\text{M}]}(y^i)] p_t^{\phi, i}(y^i \mid z_1, z_0) \quad (58)$$

Comparing with the KFE, we get data-conditional per-token rates:

$$R_t^{\phi, i}(y^i, z^i \mid z_1) = \lambda_{\text{in}}^i(t) [\delta_{[\text{M}]}(z^i) - \delta_{y^i}(z^i)] \delta_{[\text{D}]}(y^i) \\ + \lambda_{\text{um}}^i(t) [\delta_{z_1^i}(z^i) - \delta_{y^i}(z^i)] \delta_{[\text{M}]}(y^i), \quad (59)$$

which describes $[D] \rightarrow [M]$ at rate $\lambda_{\text{in}}^i(t)$ (insertion) and $[M] \rightarrow z_1^i$ at rate $\lambda_{\text{um}}^i(t)$ (unmasking).

The only thing left before we can use this target rate for training is to compute the rates $\lambda_{\text{in}}^i(t)$ and $\lambda_{\text{um}}^i(t)$ in closed form if possible. The rates $\lambda_{\text{in}}^i(t)$ and $\lambda_{\text{um}}^i(t)$ can be written in closed form in terms of the insertion density $f_{T_{\text{in}}^i}$ and the base unmasking density \dot{F}_{um}^i (and its CDF F_{um}^i), without committing to any particular functional family.

Insertion rate By definition,

$$\lambda_{\text{in}}^i(t) := \frac{f_{T_{\text{in}}^i}(t)}{\mathbb{P}(T_{\text{in}}^i > t)} = \frac{f_{T_{\text{in}}^i}(t)}{1 - F_{\text{in}}^i(t)}. \quad (60)$$

Unmasking rate Under the truncation construction Equation (35), we have for $t \geq s$:

$$\mathbb{P}(T_{\text{um}}^i > t \mid T_{\text{in}}^i = s) = 1 - \mathbb{P}(T_{\text{um}}^i \leq t \mid T_{\text{in}}^i = s) \quad (61)$$

$$= 1 - \frac{F_{\text{um}}^i(t) - F_{\text{um}}^i(s)}{1 - F_{\text{um}}^i(s)} \quad (62)$$

$$= \frac{1 - F_{\text{um}}^i(t)}{1 - F_{\text{um}}^i(s)}. \quad (63)$$

The unconditional density of T_{um}^i is

$$\begin{aligned} f_{T_{\text{um}}^i}(t) &= \int_0^t f_{T_{\text{um}}^i \mid T_{\text{in}}^i = s}(t) f_{T_{\text{in}}^i}(s) ds \\ &= \int_0^t \frac{\dot{F}_{\text{um}}^i(t)}{1 - F_{\text{um}}^i(s)} f_{T_{\text{in}}^i}(s) ds \\ &= \dot{F}_{\text{um}}^i(t) \int_0^t \frac{f_{T_{\text{in}}^i}(s)}{1 - F_{\text{um}}^i(s)} ds. \end{aligned} \quad (64)$$

The masked-state probability (the denominator of λ_{um}^i) can be written as

$$\begin{aligned} \mathbb{P}(T_{\text{in}}^i \leq t < T_{\text{um}}^i) &= \int_0^t \mathbb{P}(T_{\text{um}}^i > t \mid T_{\text{in}}^i = s) f_{T_{\text{in}}^i}(s) ds \\ &= \int_0^t (1 - \mathbb{P}(T_{\text{um}}^i \leq t \mid T_{\text{in}}^i = s)) f_{T_{\text{in}}^i}(s) ds \\ &= \int_0^t \frac{1 - F_{\text{um}}^i(t)}{1 - F_{\text{um}}^i(s)} f_{T_{\text{in}}^i}(s) ds \\ &= (1 - F_{\text{um}}^i(t)) \int_0^t \frac{f_{T_{\text{in}}^i}(s)}{1 - F_{\text{um}}^i(s)} ds. \end{aligned} \quad (65)$$

Therefore the integral cancels in the ratio, and

$$\lambda_{\text{um}}^i(t) := \frac{f_{T_{\text{um}}^i}(t)}{\mathbb{P}(T_{\text{in}}^i \leq t < T_{\text{um}}^i)} = \frac{\dot{F}_{\text{um}}^i(t)}{1 - F_{\text{um}}^i(t)}. \quad (66)$$

D.2. Likelihood under ϕ

In order to implement the gradient estimator from Equation (12), we will need to compute $p_t^{\phi,i}(z^i \mid z_1, z_0)$. From Equation (37), the conditional probability path is:

$$\begin{aligned} p_t^{\phi,i}(z^i \mid z_1, z_0) &= \mathbb{P}(T_{\text{in}}^i > t) \delta_{[D]}(z^i) + \mathbb{P}(T_{\text{in}}^i \leq t < T_{\text{um}}^i) \delta_{[M]}(z^i) (1 - \delta_{z_1^i}([D])) \\ &\quad + \mathbb{P}(T_{\text{um}}^i \leq t) \delta_{z_1^i}(z^i). \end{aligned} \quad (67)$$

For pad positions with $z_1^i = [\text{D}]$, the process stays at $[\text{D}]$ and thus $p_t^{\phi,i}(z^i | z_1, z_0) = \delta_{[\text{D}]}(z^i)$. For positions with $z_1^i \neq [\text{D}]$, under the truncated construction Equation (35) we can write the state probabilities as:

$$\mathbb{P}(T_{\text{in}}^i > t) = 1 - F_{\text{in}}^i(t), \quad (68)$$

$$\mathbb{P}(T_{\text{in}}^i \leq t < T_{\text{um}}^i) = (1 - F_{\text{um}}^i(t)) \int_0^t \frac{f_{T_{\text{in}}^i}(s)}{1 - F_{\text{um}}^i(s)} ds, \quad (69)$$

$$\mathbb{P}(T_{\text{um}}^i \leq t) = 1 - \mathbb{P}(T_{\text{in}}^i > t) - \mathbb{P}(T_{\text{in}}^i \leq t < T_{\text{um}}^i). \quad (70)$$

Substituting into the path definition yields:

$$p_t^{\phi,i}(z^i | z_1, z_0) = \mathbb{P}(T_{\text{in}}^i > t) \delta_{[\text{D}]}(z^i) + \mathbb{P}(T_{\text{in}}^i \leq t < T_{\text{um}}^i) \delta_{[\text{M}]}(z^i) (1 - \delta_{z_1^i}([\text{D}])) + \mathbb{P}(T_{\text{um}}^i \leq t) \delta_{z_1^i}(z^i). \quad (71)$$

D.3. Training

D.3.1. PROJECTED TARGET RATES

We will now apply the framework of projected rate matching from Section C to the case of variable length masked diffusion (Kim et al., 2025a). Before proceeding, recall the key notation. For variable length masked diffusion, we have an augmented space $\bar{\mathbb{Z}}_L = (\mathbb{V} \cup \{[\text{D}], [\text{M}]\})^L$ with encoder π_{enc} that removes $[\text{D}]$ tokens. The conditioning variable is $z_1 = (x_1, s_1) \in \mathbb{Z}$, where $s_1^i = i$, $i \in [\text{len}(x_1)]$ are the positions in the ground truth sequence x_1 .⁵ Equivalently, for some intermediate time, $s_t \in \mathbb{S}_{\text{len}(x_t)}$ denotes the ordered tuple of non- $[\text{D}]$ positions in z_t . That is, $s_t = (s_t^1, \dots, s_t^{\text{len}(x_t)})$ where $s_t^1 < \dots < s_t^{\text{len}(x_t)}$ are the positions in z_t that contain non- $[\text{D}]$ tokens. Then position i in the original space x_t corresponds to position s_t^i in the augmented space z_t .

For $i \in \{0, 1, \dots, \text{len}(x_t)\}$, we define the gap at position i as the set of drop positions in the augmented space between original-space positions i and $i + 1$:

$$\text{gap}_i(s_t) := \{j \in [L] : s_t^i < j < s_t^{i+1}\}, \quad (72)$$

where $s_t^0 := 0$ and $s_t^{\text{len}(x_t)+1} := L + 1$. These are the augmented positions where inserting a token would place it between positions i and $i + 1$ in the original space.

Sequence-level rates: For x_t a subsequence of x_1 , we condition on both z_1 and the position tuple $s_t \in \mathbb{S}_{\text{len}(x_t)}$ (Remark 3). The projected conditional rates (Equation (23)) are:

$$R_t^\pi(x_t, y | z_1, s_t) = \sum_{w \in \bar{\mathbb{Z}}} \pi_{\text{enc}}(y | w) R_t((x_t, s_t), w | z_1), \quad (73)$$

where we use a point-mass decoder $\pi_{\text{dec},t}(z_t | x_t, z_1, s_t) = \delta_{z_t}((x_t, s_t))$ that fixes the augmented state to $z_t = (x_t, s_t)$. For any $w = (\tilde{y}, \mathbf{r})$, the encoder can be written explicitly as:

$$\begin{aligned} \pi_{\text{enc}}(y | w) &= \delta_{f_{\text{m-drop}}(w)}(y) \\ &= \underbrace{\left(\prod_{i=1}^{\text{len}(\tilde{y})} \delta_{y^i}(\tilde{y}^{r^i}) \right)}_{\text{non-drop pos.}} \underbrace{\left(\prod_{i=1: i \notin \mathbf{r}}^L \delta_{[\text{D}]}(\tilde{y}^{r^i}) \right)}_{\text{drop positions}}. \end{aligned} \quad (74)$$

Using the assumption of per-position mixture, augmented space rates decompose as:

$$R_t((x_t, s_t), w | z_1) = \sum_{j=1}^L \delta_{(x_t, s_t)^{-j}}(w^{-j}) R_t^j(z_t^j, w^j | z_1), \quad (75)$$

⁵Technically, the empty sequence $z_0 = \emptyset$ is also present in the condition but we will suppress it for brevity.

where z_t^j denotes the token at position j in $z_t = (x_t, s_t)$. Substituting into Equation (73):

$$\begin{aligned} R_t^\pi(x_t, y|z_1, s_t) &= \sum_w \pi_{\text{enc}}(y|w) \sum_{j=1}^L \delta_{(x_t, s_t)^{-j}}(w^{-j}) R_t^j(z_t^j, w^j|z_1) \\ &= \sum_{j=1}^L \sum_{w^j} \pi_{\text{enc}}(y|(x_t, s_t)^{-j}, w^j) R_t^j(z_t^j, w^j|z_1), \end{aligned} \quad (76)$$

where we used $w = ((x_t, s_t)^{-j}, w^j)$, to mean that w equals (x_t, s_t) except at position j where it contains w^j .

Splitting the sum over $j \in [L]$ into two parts based on whether position j is a [D] position or not in $z_t = (x_t, s_t)$:

$$\begin{aligned} R_t^\pi(x_t, y|z_1, s_t) &= \underbrace{\sum_{j \in \{s_t^1, \dots, s_t^{\text{len}(x_t)}\}} \sum_{w^j} \pi_{\text{enc}}(y|(x_t, s_t)^{-j}, w^j) R_t^j(z_t^j, w^j|z_1)}_{\text{Non-[D] positions}} \\ &+ \underbrace{\sum_{j \notin \{s_t^1, \dots, s_t^{\text{len}(x_t)}\}} \sum_{w^j} \pi_{\text{enc}}(y|(x_t, s_t)^{-j}, w^j) R_t^j(\text{[D]}, w^j|z_1)}_{\text{[D] positions}}. \end{aligned} \quad (77)$$

For non-[D] positions, reindexing with $j = s_t^i$ for $i \in [\text{len}(x_t)]$, and noting that $z_t^{s_t^i} = x_t^i$:

$$\begin{aligned} \text{Non-[D]} &= \sum_{i=1}^{\text{len}(x_t)} \sum_{w^{s_t^i}} \pi_{\text{enc}}(y|(x_t, s_t)^{-s_t^i}, w^{s_t^i}) R_t^{s_t^i}(x_t^i, w^{s_t^i}|z_1) \\ &\stackrel{(1)}{=} \sum_{i=1}^{\text{len}(x_t)} \sum_{w^{s_t^i}} \delta_y((x_t^{-i}, w^{s_t^i})) R_t^{s_t^i}(x_t^i, w^{s_t^i}|z_1) \\ &= \sum_{i=1}^{\text{len}(x_t)} \delta_{y^{-i}}(x_t^{-i}) R_t^{s_t^i}(x_t^i, y^i|z_1) \end{aligned} \quad (78)$$

$$\stackrel{(2)}{=} \sum_{i=1}^{\text{len}(x_t)} \delta_{y^{-i}}(x_t^{-i}) \lambda_{\text{um}, t}^{s_t^i}(z_1) \left[\delta_{z_1^{s_t^i}}(y^i) - \delta_{x_t^i}(y^i) \right] \delta_{\text{[M]}}(x_t^i) \quad (79)$$

where (1) uses the encoder definition Equation (74), and (2) substitutes the target augmented rates from Equation (59).

For the [D] positions (where $j \notin \{s_t^1, \dots, s_t^{\text{len}(x_t)}\}$), we have $z_t^j = \text{[D]}$:

$$\begin{aligned} \text{[D] pos.} &= \sum_{j \notin s_t} \sum_{w^j} \pi_{\text{enc}}(y|(x_t, s_t)^{-j}, w^j) R_t^j(\text{[D]}, w^j|z_1) \\ &\stackrel{(1)}{=} \sum_{j \notin s_t} \pi_{\text{enc}}(y|(x_t, s_t)^{-j}, \text{[M]}) \lambda_{\text{in}, t}^j(z_1) \\ &\stackrel{(2)}{=} \sum_{i=0}^{\text{len}(x_t)} \delta_y((x_t^{1:i}, \text{[M]}, x_t^{i+1:\text{len}(x_t)})) \sum_{j \in \text{gap}_i(s_t)} \lambda_{\text{in}, t}^j(z_1), \end{aligned} \quad (80)$$

where (1) uses the augmented target rates (Equation (59)): $R_t^j(\text{[D]}, w^j|z_1) = \lambda_{\text{in}, t}^j(z_1) \delta_{\text{[M]}}(w^j)$, so only $w^j = \text{[M]}$ contributes (insertion). For (2), when $w^j = \text{[M]}$ at position $j \in \text{gap}_i(s_t)$, the encoder requires $y = f_{\text{rm-drop}}((x_t, s_t)^{-j}, \text{[M]})$ to have the form $(x_t^{1:i}, \text{[M]}, x_t^{i+1:\text{len}(x_t)})$, inserting [M] at position i in the original space.

We can express the non-drop and drop positions rates compactly by defining per-position rate components. For unmasking at position $i \in [\text{len}(x_t)]$:

$$R_{\text{um}}^{\pi, i}(x_t^i, y^i|z_1, s_t) := \lambda_{\text{um}, t}^{s_t^i}(z_1) \left[\delta_{z_1^{s_t^i}}(y^i) - \delta_{x_t^i}(y^i) \right] \delta_{\text{[M]}}(x_t^i), \quad (81)$$

and for insertion at gap $i \in \{0, 1, \dots, \text{len}(x_t)\}$:

$$R_{\text{in}}^{\pi,i}([\mathbf{M}]|z_1, s_t) := \sum_{j \in \text{gap}_i(s_t)} \lambda_{\text{in},t}^j(z_1). \quad (82)$$

Therefore, the projected rates can be written as per-position mixture:

$$\begin{aligned} R_t^\pi(x_t, y|z_1, s_t) &= \sum_{i=1}^{\text{len}(x_t)} \delta_{y^{-i}}(x_t^{-i}) R_{\text{um}}^{\pi,i}(x_t^i, y^i|z_1, s_t) \\ &+ \sum_{i=0}^{\text{len}(x_t)} \delta_y((x_t^{1:i}, [\mathbf{M}], x_t^{i+1:\text{len}(x_t)})) R_{\text{in}}^{\pi,i}([\mathbf{M}]|z_1, s_t). \end{aligned} \quad (83)$$

Remark 4 (Relationship to marginalized rates:). The projected rate $R_t^\pi(x_t, y|z_1, s_t)$ conditioned on both z_1 and s_t is related to the marginalized version by:

$$R_t^\pi(x_t, y|z_1) = \sum_{s_t \in \mathbb{S}_{\text{len}(x_t)}} p_{t|z_1}(s_t|x_t, z_1) R_t^\pi(x_t, y|z_1, s_t). \quad (84)$$

Using Proposition 5, we can learn both ϕ and θ by minimizing

$$\mathcal{L}^{\theta,\phi} = \mathbb{E}_{X_t, Z_1, S_t} D_F(R_t^{\pi,\phi}(X_t, \cdot|Z_1, S_t), R_t^\theta(X_t, \cdot)), \quad (85)$$

where $Z_1 \sim p_{\text{data}}$ and $(X_t, S_t) \sim p_{t|Z_1}^\phi$.

D.4. Loss function

We parameterize the generator rates $R_t^\theta(x_t, y)$ using per-position mixture

$$R^\theta(x_t, y) = \sum_{i=1}^{\text{len}(x_t)} \delta_{x_t^{-i}}(y^{-i}) \left[R_{\text{um},t}^{\theta,i}(x_t, y^i) + R_{\text{in},t}^{\theta,i}(x_t, [\mathbf{M}]) \right], \quad (86)$$

where $R_{\text{um},t}^{\theta,i}(x, y^i) = \lambda_{\text{um},t}^{\theta,i}(x) K_t^{\theta,i}(y^i|x_t)$ and $R_{\text{in},t}^{\theta,i}(x, [\mathbf{M}]) = \lambda_{\text{in},t}^{\theta,i}(x)$.

We can now substitute the parametric rates into Equation (85) to get the training objective.

$$\mathcal{L}^{\theta,\phi}(x_t, z_1, s_t) = \sum_{y \in \mathcal{Y}(x_t)} \left[R_t^{\pi,\phi}(x_t, y|z_1, s_t) \log \frac{R_t^{\pi,\phi}(x_t, y|z_1, s_t)}{R_t^\theta(x_t, y)} - R_t^{\pi,\phi}(x_t, y|z_1, s_t) + R_t^\theta(x_t, y) \right], \quad (87)$$

where $\mathcal{Y}(x_t)$ is the set of sequences y that differ from x_t at exactly one position. Note that both terms depend on learnable parameters (ϕ and θ respectively), so there are no constant terms to drop.

Substituting the two-sum form Equation (83), we obtain:

$$\begin{aligned} \mathcal{L}^{\theta,\phi}(x_t, z_1, s_t) &= \mathbb{E}_{t, z_1, z_t \sim p_{t|z_1}^\phi} \left[\sum_{i=1}^{\text{len}(x_t)} \delta_{[\mathbf{M}]}(x_t^i) \sum_{y^i \in \mathbb{V}} \left(R_{\text{um}}^{\pi,\phi,i}(x_t^i, y^i|z_1, s_t) \log \frac{R_{\text{um}}^{\pi,\phi,i}(x_t^i, y^i|z_1, s_t)}{R_{\text{um},t}^{\theta,i}(x_t, y^i)} \right. \right. \\ &\quad \left. \left. - R_{\text{um}}^{\pi,\phi,i}(x_t^i, y^i|z_1, s_t) + R_{\text{um},t}^{\theta,i}(x_t, y^i) \right) \right. \\ &\quad \left. + \sum_{i=0}^{\text{len}(x_t)} \left(R_{\text{in}}^{\pi,\phi,i}([\mathbf{M}]|z_1, s_t) \log \frac{R_{\text{in}}^{\pi,\phi,i}([\mathbf{M}]|z_1, s_t)}{R_{\text{in},t}^{\theta,i}(x_t, [\mathbf{M}])} \right. \right. \\ &\quad \left. \left. - R_{\text{in}}^{\pi,\phi,i}([\mathbf{M}]|z_1, s_t) + R_{\text{in},t}^{\theta,i}(x_t, [\mathbf{M}]) \right) \right]. \end{aligned}$$

Expanding using the definitions of $R_{\text{um}}^{\pi,\phi,i}$, $R_{\text{in}}^{\pi,\phi,i}$, $R_{\text{um},t}^{\theta,i}$, $R_{\text{in},t}^{\theta,i}$ produces the final expression for the loss as stated in Equation (11).

$$\begin{aligned} \mathcal{L}^{\theta,\phi} = \mathbb{E}_{t,z_1,z_t \sim p_{t|z_1}^\phi} & \left[\sum_{i=1}^{\text{len}(x_t)} \delta_{[M]}(x_t^i) \left(\lambda_{\text{um},t}^{\phi,s_t^i}(z_1) \log \frac{\lambda_{\text{um},t}^{\phi,s_t^i}(z_1)}{\lambda_{\text{um},t}^{\theta,i}(x_t) K_t^{\theta,i}(z_1^{s_t^i} | x_t)} \right. \right. \\ & \left. \left. - \lambda_{\text{um},t}^{\phi,s_t^i}(z_1) + \lambda_{\text{um},t}^{\theta,i}(x_t) \right) \right. \\ & + \sum_{i=0}^{\text{len}(x_t)} \left(\left(\sum_{j \in \text{gap}_i(s_t)} \lambda_{\text{in},t}^{\phi,j}(z_1) \right) \log \frac{\sum_{j \in \text{gap}_i(s_t)} \lambda_{\text{in},t}^{\phi,j}(z_1)}{\lambda_{\text{in},t}^{\theta,i}(x_t)} \right. \\ & \left. \left. - \left(\sum_{j \in \text{gap}_i(s_t)} \lambda_{\text{in},t}^{\phi,j}(z_1) \right) + \lambda_{\text{in},t}^{\theta,i}(x_t) \right) \right]. \end{aligned} \quad (88)$$

D.5. Gradient computation

In order to take gradient w.r.t ϕ present in the expectation, we can use REINFORCE leave one out as follows. We want to compute the following gradient:

$$\nabla_\phi \mathbb{E}_{z \sim p^\phi} f^\phi(z)$$

A simple REINFORCE style estimate will be:

$$\nabla_\phi \mathbb{E}_{z \sim p^\phi} f^\phi(z) = \mathbb{E}_{z \sim p^\phi} [\nabla_\phi \log p^\phi(z) f^\phi(z) + \nabla_\phi f^\phi(z)]. \quad (89)$$

The first term will be high variance. We can introduce GRPO style baseline for the first term. Say we have n samples z_1, \dots, z_n from p^ϕ . Then we can define the baseline as:

$$b_i = \frac{1}{n-1} \sum_{j \neq i} f^\phi(z_j).$$

We can then do a multi-sample MC estimate with this baseline where each z_i plays the role of z once, giving us the following estimate for the first term:

$$\begin{aligned} & \frac{1}{n} \sum_{i=1}^n [f^\phi(z_i) - b_i] \nabla_\phi \log p^\phi(z_i) \\ & = \frac{1}{n} \sum_{i=1}^n \left[f^\phi(z_i) - \left(\frac{1}{n-1} \sum_{j \neq i} f^\phi(z_j) \right) \right] \nabla_\phi \log p^\phi(z_i) \end{aligned}$$

Using $n = 2$ we get the following simple estimator:

$$\begin{aligned} & \frac{1}{2} \sum_{i=1}^2 \left[f^\phi(z_i) - \left(\frac{1}{2-1} \sum_{j \neq i} f^\phi(z_j) \right) \right] \nabla_\phi \log p^\phi(z_i) \\ & = \frac{1}{2} \sum_{i=1}^2 \left[f^\phi(z_i) - \sum_{j \neq i} f^\phi(z_j) \right] \nabla_\phi \log p^\phi(z_i) \\ & = \frac{1}{2} \left\{ [f^\phi(z_1) - f^\phi(z_2)] \nabla_\phi \log p^\phi(z_1) + [f^\phi(z_2) - f^\phi(z_1)] \nabla_\phi \log p^\phi(z_2) \right\} \\ & = \frac{1}{2} \left\{ [f^\phi(z_1) - f^\phi(z_2)] \nabla_\phi \log p^\phi(z_1) - [f^\phi(z_1) - f^\phi(z_2)] \nabla_\phi \log p^\phi(z_2) \right\} \\ & = \frac{1}{2} [f^\phi(z_1) - f^\phi(z_2)] [\nabla_\phi \log p^\phi(z_1) - \nabla_\phi \log p^\phi(z_2)] \end{aligned}$$

Plugging this back into Equation (89) we get the following estimator for the gradient:

$$\nabla_{\phi} \mathbb{E}_{z \sim p^{\phi}} f^{\phi}(z) \approx \frac{1}{2} [f^{\phi}(z_1) - f^{\phi}(z_2)] [\nabla_{\phi} \log p^{\phi}(z_1) - \nabla_{\phi} \log p^{\phi}(z_2)] + \frac{1}{2} [\nabla_{\phi} f^{\phi}(z_1) + \nabla_{\phi} f^{\phi}(z_2)]$$

D.5.1. FULL GRADIENT ESTIMATOR FOR TWO PARAMETER SETS

If we have $f^{\phi, \theta}(z)$ that depends on two sets of parameters (ϕ, θ) where $z \sim p^{\phi}$, we need to compute:

$$\nabla_{(\phi, \theta)} \mathbb{E}_{z \sim p^{\phi}} f^{\phi, \theta}(z).$$

The key observation is that the distribution p^{ϕ} only depends on ϕ and not on θ . Therefore:

Gradient w.r.t. θ : Since p^{ϕ} doesn't depend on θ , we can move the gradient inside the expectation:

$$\nabla_{\theta} \mathbb{E}_{z \sim p^{\phi}} f^{\phi, \theta}(z) = \mathbb{E}_{z \sim p^{\phi}} \nabla_{\theta} f^{\phi, \theta}(z) \approx \frac{1}{2} [\nabla_{\theta} f^{\phi, \theta}(z_1) + \nabla_{\theta} f^{\phi, \theta}(z_2)].$$

This is a simple Monte Carlo average of the direct gradients.

Gradient w.r.t. ϕ : Here we still need REINFORCE since p^{ϕ} depends on ϕ :

$$\begin{aligned} \nabla_{\phi} \mathbb{E}_{z \sim p^{\phi}} f^{\phi, \theta}(z) &= \mathbb{E}_{z \sim p^{\phi}} [\nabla_{\phi} \log p^{\phi}(z) f^{\phi, \theta}(z) + \nabla_{\phi} f^{\phi, \theta}(z)] \\ &\approx \frac{1}{2} [f^{\phi, \theta}(z_1) - f^{\phi, \theta}(z_2)] [\nabla_{\phi} \log p^{\phi}(z_1) - \nabla_{\phi} \log p^{\phi}(z_2)] \\ &\quad + \frac{1}{2} [\nabla_{\phi} f^{\phi, \theta}(z_1) + \nabla_{\phi} f^{\phi, \theta}(z_2)]. \end{aligned}$$

The full gradient estimator is then:

$$\nabla_{(\phi, \theta)} \mathbb{E}_{z \sim p^{\phi}} f^{\phi, \theta}(z) \approx \begin{pmatrix} \frac{1}{2} [f^{\phi, \theta}(z_1) - f^{\phi, \theta}(z_2)] [\nabla_{\phi} \log p^{\phi}(z_1) - \nabla_{\phi} \log p^{\phi}(z_2)] \\ \quad + \frac{1}{2} [\nabla_{\phi} f^{\phi, \theta}(z_1) + \nabla_{\phi} f^{\phi, \theta}(z_2)] \\ \frac{1}{2} [\nabla_{\theta} f^{\phi, \theta}(z_1) + \nabla_{\theta} f^{\phi, \theta}(z_2)] \end{pmatrix}. \quad (90)$$

D.5.2. SCHEDULE REGULARIZATION

If ϕ is optimized jointly with θ , Equation (11) admits degenerate solutions where the insertion/unmasking-time distributions place excessive probability mass near the endpoints $t = 0$ or $t = 1$ (e.g., delaying most events until $t \approx 1$). This suppresses the (rate-weighted) prediction term in Equation (11) and allows the model hazards to match near-zero target hazards with negligible cost. To discourage such degenerate schedules, we add a sequence level schedule prior, which acts as a regularizer on the target schedule.

We add a loss term to regularize the *mixture CDF across positions* to be close to a straight line $F(t) = t$. Intuitively, this encourages the marginal event time of a uniformly sampled position to be approximately $\mathcal{U}[0, 1]$, discouraging excessive mass near $t = 0$ or $t = 1$ without prescribing a particular per-position shape. The mixture CDFs over positions is defined as:

$$\bar{F}_{\text{in}}^{\phi}(t) := \frac{1}{L} \sum_{i=1}^L F_{\text{in}}^{\phi, i}(t), \quad \bar{F}_{\text{um}}^{\phi}(t) := \frac{1}{L} \sum_{i=1}^L F_{\text{um}}^{\phi, i}(t), \quad (91)$$

where L is the sequence length. We then add a penalty encouraging $\bar{F}_{\text{in}}^{\phi}(t) \approx t$ and $\bar{F}_{\text{um}}^{\phi}(t) \approx t$, on a grid $\{t_k\}_{k=1}^K \subset (0, 1)$:

$$\mathcal{L}_{\text{reg}}(\phi) = \sum_{k=1}^K w_k \left(\bar{F}_{\text{in}}^{\phi}(t_k) - t_k \right)^2 + \sum_{k=1}^K w_k \left(\bar{F}_{\text{um}}^{\phi}(t_k) - t_k \right)^2, \quad (92)$$

which approximates the continuous-time objective $\int_0^1 (\bar{F}_{\text{in}}^{\phi}(t) - t)^2 + (\bar{F}_{\text{um}}^{\phi}(t) - t)^2 dt$.

Additionally, we penalize each position separately to stay away from concentrating mass near the endpoints. For this, we fix a small time cutoff $t_\epsilon \in (0, 1/2)$ and tolerance $\delta \in (0, 1)$, and enforce:

$$F_{\text{in}}^{\phi,i}(t_\epsilon) \leq \delta, \quad 1 - F_{\text{in}}^{\phi,i}(1 - t_\epsilon) \leq \delta, \quad (93)$$

$$G_{\text{um}}^{\phi,i}(t_\epsilon) \leq \delta, \quad 1 - G_{\text{um}}^{\phi,i}(1 - t_\epsilon) \leq \delta, \quad (94)$$

implemented via soft hinge penalties. In the implementation, we use $t_\epsilon = 0.01$ and $\delta = 0.01$.

D.5.3. KUMARASWAMY SCHEDULES

We use Kumaraswamy schedules for the insertion and unmasking times: $T_{\text{in}}^i \sim \text{Kumaraswamy}(a_{\text{in}}, b_{\text{in}})$ and $U^i \sim \text{Kumaraswamy}(a_{\text{um}}, b_{\text{um}})$ on $[0, 1]$. Then

$$F_{\text{in}}^i(t) = 1 - (1 - t^{a_{\text{in}}})^{b_{\text{in}}}, \quad f_{T_{\text{in}}^i}(t) = a_{\text{in}} b_{\text{in}} t^{a_{\text{in}}-1} (1 - t^{a_{\text{in}}})^{b_{\text{in}}-1}, \quad \mathbb{P}(T_{\text{in}}^i > t) = (1 - t^{a_{\text{in}}})^{b_{\text{in}}}, \quad (95)$$

$$F_{\text{um}}^i(t) = 1 - (1 - t^{a_{\text{um}}})^{b_{\text{um}}}, \quad \dot{F}_{\text{um}}^i(t) = a_{\text{um}} b_{\text{um}} t^{a_{\text{um}}-1} (1 - t^{a_{\text{um}}})^{b_{\text{um}}-1}, \quad 1 - F_{\text{um}}^i(t) = \mathbb{P}(U^i > t) = (1 - t^{a_{\text{um}}})^{b_{\text{um}}}. \quad (96)$$

By Equation (35), the induced conditional distribution of T_{um}^i on $[s, 1]$ is

$$\mathbb{P}(T_{\text{um}}^i \leq t \mid T_{\text{in}}^i = s) = \delta(t \geq s) \left[1 - \frac{1 - F_{\text{um}}^i(t)}{1 - F_{\text{um}}^i(s)} \right] = \delta(t \geq s) \left[1 - \frac{(1 - t^{a_{\text{um}}})^{b_{\text{um}}}}{(1 - s^{a_{\text{um}}})^{b_{\text{um}}}} \right], \quad (97)$$

$$f_{T_{\text{um}}^i \mid T_{\text{in}}^i = s}(t) = \delta(t \geq s) \frac{\dot{F}_{\text{um}}^i(t)}{1 - F_{\text{um}}^i(s)} = \delta(t \geq s) \frac{a_{\text{um}} b_{\text{um}} t^{a_{\text{um}}-1} (1 - t^{a_{\text{um}}})^{b_{\text{um}}-1}}{(1 - s^{a_{\text{um}}})^{b_{\text{um}}}}. \quad (98)$$

Plugging into Equations (60) and (66) yields

$$\lambda_{\text{in}}^i(t) = \frac{a_{\text{in}} b_{\text{in}} t^{a_{\text{in}}-1}}{1 - t^{a_{\text{in}}}} \quad \text{and} \quad \lambda_{\text{um}}^i(t) = \frac{a_{\text{um}} b_{\text{um}} t^{a_{\text{um}}-1}}{1 - t^{a_{\text{um}}}}. \quad (99)$$

For $t \in [0, 1]$,

$$\mathbb{P}(T_{\text{in}}^i > t) = (1 - t^{a_{\text{in}}})^{b_{\text{in}}}, \quad (100)$$

$$\mathbb{P}(T_{\text{in}}^i \leq t < T_{\text{um}}^i) = (1 - t^{a_{\text{um}}})^{b_{\text{um}}} \int_0^t \frac{a_{\text{in}} b_{\text{in}} s^{a_{\text{in}}-1} (1 - s^{a_{\text{in}}})^{b_{\text{in}}-1}}{(1 - s^{a_{\text{um}}})^{b_{\text{um}}}} ds, \quad (101)$$

$$\mathbb{P}(T_{\text{um}}^i \leq t) = 1 - (1 - t^{a_{\text{in}}})^{b_{\text{in}}} - \mathbb{P}(T_{\text{in}}^i \leq t < T_{\text{um}}^i). \quad (102)$$

To see that $\mathbb{P}(T_{\text{in}}^i \leq t < T_{\text{um}}^i)$ is a valid probability, rewrite it using the law of total probability:

$$\mathbb{P}(T_{\text{in}}^i \leq t < T_{\text{um}}^i) = \int_0^t f_{T_{\text{in}}^i}(s) \mathbb{P}(T_{\text{um}}^i > t \mid T_{\text{in}}^i = s) ds = \int_0^t f_{T_{\text{in}}^i}(s) \frac{1 - F_{\text{um}}^i(t)}{1 - F_{\text{um}}^i(s)} ds.$$

For $s \leq t$, the survival function is monotone so $1 - F_{\text{um}}^i(t) \leq 1 - F_{\text{um}}^i(s)$, hence the ratio is in $[0, 1]$ and the integral is in $[0, F_{\text{in}}^i(t)] \subseteq [0, 1]$. In general, the integral does not simplify to elementary functions, but it admits closed forms in certain special cases.

Special case $a_{\text{in}} = a_{\text{um}} = a$ If $a_{\text{in}} = a_{\text{um}} = a$, the integral $I(t) := \int_0^t \frac{a_{\text{in}} b_{\text{in}} s^{a_{\text{in}}-1} (1 - s^{a_{\text{in}}})^{b_{\text{in}}-1}}{(1 - s^{a_{\text{um}}})^{b_{\text{um}}}} ds$ simplifies to

$$\begin{aligned} I(t) &= \int_0^t a b_{\text{in}} s^{a-1} (1 - s^a)^{b_{\text{in}}-b_{\text{um}}-1} ds \\ &\stackrel{u=s^a}{=} b_{\text{in}} \int_0^{t^a} (1 - u)^{b_{\text{in}}-b_{\text{um}}-1} du \\ &= \begin{cases} \frac{b_{\text{in}}}{b_{\text{in}} - b_{\text{um}}} [1 - (1 - t^a)^{b_{\text{in}}-b_{\text{um}}}], & b_{\text{in}} \neq b_{\text{um}}, \\ -b_{\text{in}} \ln(1 - t^a), & b_{\text{in}} = b_{\text{um}}. \end{cases} \end{aligned} \quad (103)$$

D.5.4. PROBABILITY OF AN ORDER UNDER KUMARASWAMY SCHEDULE

For a sequence of length L , let $\{T^i\}_{i=1}^L$ denote the event times, one for each position, such that $T^i \leq 1$ almost surely. Let $\pi : [L] \rightarrow [L]$ be a bijection such that $T^{\pi(1)} < T^{\pi(2)} < \dots < T^{\pi(L)}$, then π is an order over the positions induced by the event times.

Interestingly, we get a nice closed form expression for orders under the Kumaraswamy schedule if we fix a for all positions (special case 2, mentioned in Section D.5.3).

Proposition 6 (Probability of an order under Kumaraswamy Schedule). *For $t \in [0, 1]$, let the CDF of the event time for the i -th position be given by the Kumaraswamy distribution with parameters a and b^i , i.e., $F_{T^i}(t) = 1 - (1 - t^a)^{b^i}$, then the probability of an order π is given by:*

$$\mathbb{P}(\pi) = \prod_{i=1}^L \frac{b^{\pi(i)}}{\sum_{j=i}^L b^{\pi(j)}} \quad (104)$$

Proof. The proof is straightforward and follows directly from the following two results.

1. If the event times T^i are independent and have exponential distribution with parameter b^i , then the probability of an order π is given by:

$$\mathbb{P}(\pi) = \prod_{i=1}^L \frac{b^{\pi(i)}}{\sum_{j=i}^L b^{\pi(j)}}$$

2. Let N_t be a nonhomogeneous Poisson process with hazard rate of the form $\lambda(t) = b\beta(t)$. Then \bar{N}_u is a homogeneous Poisson process with warped time $u = \int_0^t \beta(s)ds$. Let $U_1 = \inf\{u : \bar{N}_u = 1\}$, be the first arrival time of the homogeneous Poisson process.

□

D.6. Sampling

The generator network predicts learnable hazard rates $\lambda_{\text{in},t}^{\theta,i}(x_t)$ for insertion at gap position i and $\lambda_{\text{um},t}^{\theta,i}(x_t)$ for unmasking at masked position i , along with the token distribution $K^{\theta,i}(\cdot|x_t)$.

We use a simple τ -leaping sampler that allows for larger time steps by sampling the number of events (insertions/unmaskings) in each interval $[t_n, t_{n+1})$ from a Poisson distribution. For small $\tau = t_{n+1} - t_n$, the first-order approximation gives Poisson intensities $\int_{t_n}^{t_{n+1}} \lambda_s ds \approx \lambda_{t_n} \cdot \tau$.

Algorithm 3 Training for LFlexMDM (Detailed)

Require: Dataset \mathcal{D} , generator parameters θ , target rate parameters ϕ , learning rate η

```

1: function TRUNCSAMPLE( $s, F$ ) // Sample from  $F$  truncated to  $[s, 1]$ 
2:    $u \sim \mathcal{U}(0, 1)$ 
3:   return  $F^{-1}(u \cdot (1 - F(s)) + F(s))$ 
4:
5: while not converged do
6:   Sample  $z_1 \sim p_{\text{data}}$  //  $z_1 \in \bar{\mathbb{Z}}$ : padded with [D] tokens
7:   Sample  $t \sim \mathcal{U}(0, 1)$  // Diffusion time
8:    $(a_{\text{in}}^{\phi, i}, b_{\text{in}}^{\phi, i}, a_{\text{um}}^{\phi, i}, b_{\text{um}}^{\phi, i}) \leftarrow \phi(z_1)$  // Kumaraswamy params per position
9:   for  $k = 1$  to  $2$  do
10:    for  $i = 1$  to  $L$  do
11:      $T_{\text{in}}^{i, (k)} \sim F_{\text{in}}^{\phi, i}$  // Insertion time
12:      $T_{\text{um}}^{i, (k)} \leftarrow \text{TRUNCSAMPLE}(T_{\text{in}}^{i, (k)}, F_{\text{um}}^{\phi, i})$  // Unmasking after insertion
13:      $z_t^{i, (k)} \leftarrow \begin{cases} [\text{D}] & T_{\text{in}}^{i, (k)} > t \\ [\text{M}] & T_{\text{in}}^{i, (k)} \leq t < T_{\text{um}}^{i, (k)} \\ z_1^i & T_{\text{um}}^{i, (k)} \leq t \end{cases}$ 
14:    end for
15:     $x_t^{(k)}, s_t^{(k)} \leftarrow f_{\text{contract}}(z_t^{(k)})$  // Use the bijection to get positions
16:     $\mathcal{L}_k \leftarrow \mathcal{L}_{\text{um}}^{\phi, \theta} + \mathcal{L}_{\text{in}}^{\phi, \theta}$  // Compute loss (Equation (11))
17:  end for
18:  // Combine REINFORCE (with stop-grad) and pathwise gradients:
19:   $\mathcal{L} \leftarrow \frac{1}{2} \left[ (\text{sg}(\mathcal{L}_1) - \text{sg}(\mathcal{L}_2)) \log \frac{p_{t|z_1}^{\phi}(z_t^{(1)})}{p_{t|z_1}^{\phi}(z_t^{(2)})} + \mathcal{L}_1 + \mathcal{L}_2 \right]$ 
20:   $(\theta, \phi) \leftarrow (\theta, \phi) - \eta \nabla_{(\theta, \phi)} \mathcal{L}$  // Single backward pass
21: end while

```

Algorithm 4 Tau-Leaping Sampling for LFlexMDM

```

1: Input: Time steps  $0 = t_0 < t_1 < \dots < t_N = 1$ , nucleus  $p$ , confidence function  $c$ 
2: Initialize  $x_0 = \emptyset$  (empty sequence)
3: for  $n = 0$  to  $N - 1$  do
4:    $\tau \leftarrow t_{n+1} - t_n$ 
5:   Predict  $\lambda_{\text{in},t_n}^{\theta,i}(x_n)$ ,  $\lambda_{\text{um},t_n}^{\theta,i}(x_n)$ , and  $K^{\theta,i}(\cdot|x_n)$  from network  $\theta$ 
6:    $x_{n+1} \leftarrow x_n$ 
7:   for each gap position  $i = 0$  to  $\text{len}(x_n)$  do
8:      $N_{\text{in}}^i \sim \text{Poisson}(\lambda_{\text{in},t_n}^{\theta,i}(x_n) \cdot \tau)$ 
9:     if  $N_{\text{in}}^i > 0$  then
10:       Insert  $N_{\text{in}}^i$  masks at gap position  $i$  in  $x_{n+1}$ 
11:     end if
12:   end for
13:   for each masked position  $i$  in  $x_{n+1}$  do
14:     for each token  $y \in \mathbb{V}$  do
15:        $N_{\text{um}}^{i,y} \sim \text{Poisson}(\lambda_{\text{um},t_n}^{\theta,i}(x_n) \cdot K^{\theta,i}(y|x_n) \cdot \tau)$ 
16:     end for
17:     //candidate unmask locations
18:      $u_i \leftarrow \delta(\sum_{y \in \mathbb{V}} N_{\text{um}}^{i,y} > 0)$ 
19:   end for
20:   if confidence enabled then
21:     // select  $\{|i : u_i=1\}$  locations with largest confidence  $c_i$ 
22:      $u \leftarrow \text{SELECT}(\sum_i u_i; c(K^\theta, \lambda^\theta))$ 
23:   end if
24:   for each masked position  $i$  in  $x_{n+1}$  with  $u_i = 1$  do
25:      $x_{n+1}^i \stackrel{\text{nucleus}(p)}{\sim} K^{\theta,i}(\cdot|x_n)$ 
26:   end for
27: end for
28: return  $x_N$ 

```

D.7. Truncation vs Rescaling

We need to sample two event times T_{in} and T_{um} with a constraint $T_{\text{in}} < T_{\text{um}}$. For constructing a learnable schedule for this we need to parameterize

$$\mathbb{P}(T_{\text{in}} \leq t), \quad \text{and} \quad \mathbb{P}(T_{\text{um}} \leq t \mid T_{\text{in}} = s).$$

It is straightforward to parameterize $\mathbb{P}(T_{\text{in}} \leq t)$ using any monotonic function $F_{\text{in}}(t)$ that satisfies $F_{\text{in}}(0) = 0$ and $F_{\text{in}}(1) = 1$. However, for $\mathbb{P}(T_{\text{um}} \leq t \mid T_{\text{in}} = s)$, we have two easy choices. We can take a base monotonic function $F_{\text{um}}(t)$ and either **truncate** or **rescale** it to $[s, 1]$, where,

$$\begin{aligned} \text{truncate:} \quad \mathbb{P}(T_{\text{um}} \leq t \mid T_{\text{in}} = s) &= \frac{F_{\text{um}}(t) - F_{\text{um}}(s)}{1 - F_{\text{um}}(s)}, \\ \text{rescale:} \quad \mathbb{P}(T_{\text{um}} \leq t \mid T_{\text{in}} = s) &= F_{\text{um}}\left(\frac{t-s}{1-s}\right). \end{aligned}$$

However, the unmasking hazard rate in Equation (66) simplifies to a closed form expression only for the truncated case. Figure 8 shows a comparison of truncated and rescaled Kumaraswamy CDFs.

E. Details of the experiment setup

E.1. Graph Traversal

Dataset. We use the star graphs dataset from Patel et al. (2025b) obtained from Hugging Face Hub.

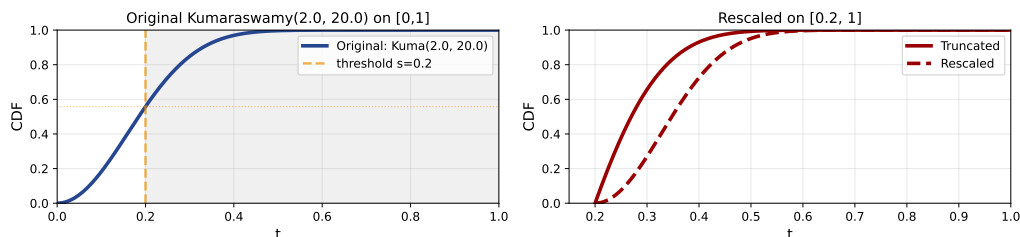


Figure 8. Comparison of truncated and rescaled Kumaraswamy CDFs for different parameter values.

Model. Following the setup in Kim et al. (2025a), we use a linear layer for modeling the insertion lengths in each gap for FlexMDM. For LMFlexMDM, we use two MLP layers for modeling the parameters of the learned target rates.

Hyperparameters. Table 5 shows the hyperparameters for the star graphs experiments.

Model	lr	wt decay	train_steps	sampling_steps	confidence
FlexMDM	10^{-4}	10^{-2}	80,000	500	×
LMFlexMDM	10^{-4}	10^{-2}	80,000	500	×

Table 4. Hyperparameters for star graphs experiments.

E.2. Molecule Generation

Hyperparameters. Table 5 shows the hyperparameters for the molecule generation experiments.

Model	lr	wt decay	train_steps	sampling_steps	confidence
FlexMDM	10^{-4}	10^{-2}	50,000	1024	×
LMFlexMDM	10^{-4}	10^{-2}	50,000	1024	✓

Table 5. Hyperparameters for star graphs experiments.

F. Additional Results and Analyses

Table 7 shows the results for *de novo* small molecule generation with additional nucleus-sampling p values, as well as a shared-backbone implementation.

F.1. Flexibility vs Stability

Figure 9 shows the loss comparison for the hard star graph traversal task with and without fixing target unmasking rate ($b_{um} = 1$). As seen, fixing the target unmasking rate stabilizes the training significantly, and as shown in Table 6, it also improves the overall performance of the final generator.

F.2. Star Graph Traversal

Table 6 shows the token accuracy along with exact match for the star graph traversal task.

F.2.1. EXAMPLES: GENERATION ORDER

Fixing target unmasking rate ($b_{um} = 1$) Figure 9 shows the loss comparison for the hard star graph traversal task with and without fixing target unmasking rate ($b_{um} = 1$). As seen, fixing the target unmasking rate stabilizes the training significantly, and as shown in Table 6, it also improves the overall performance of the final generator.

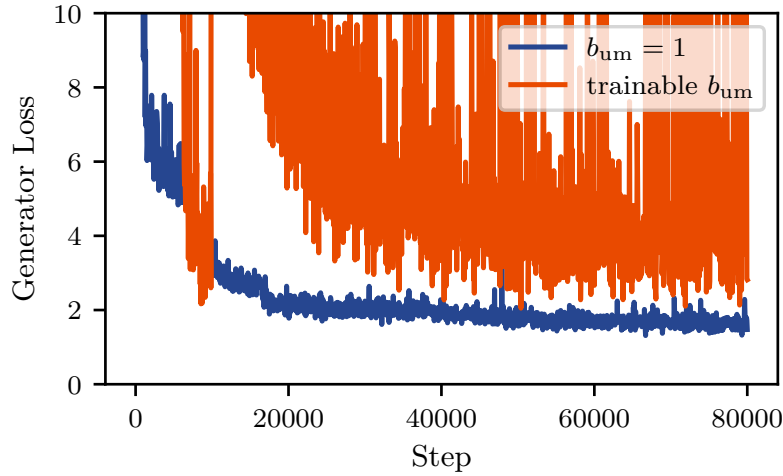


Figure 9. Loss comparison for the hard star graph traversal task with and without fixing target unmasking rate ($b_{um} = 1$). The erratic dynamics of a fully unconstrained set of target rates motivates freezing b_{um} .

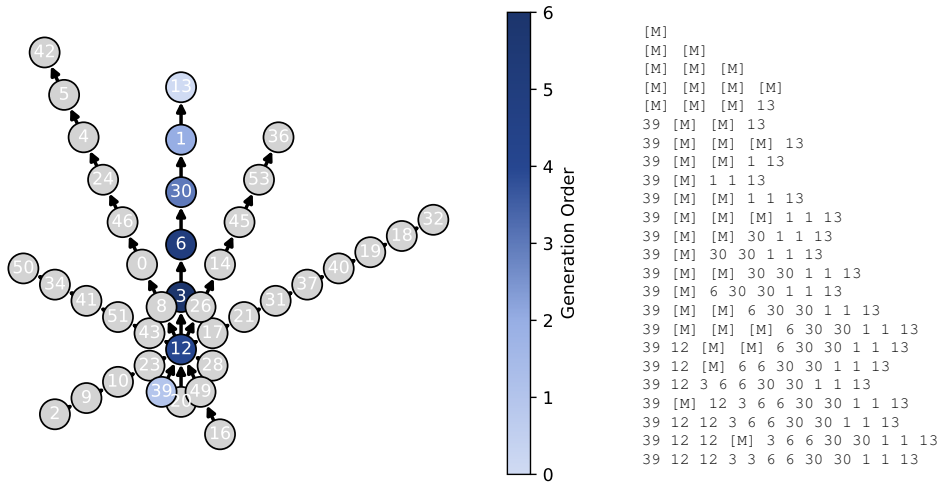


Figure 10. Example of generation order for LFlexMDM.

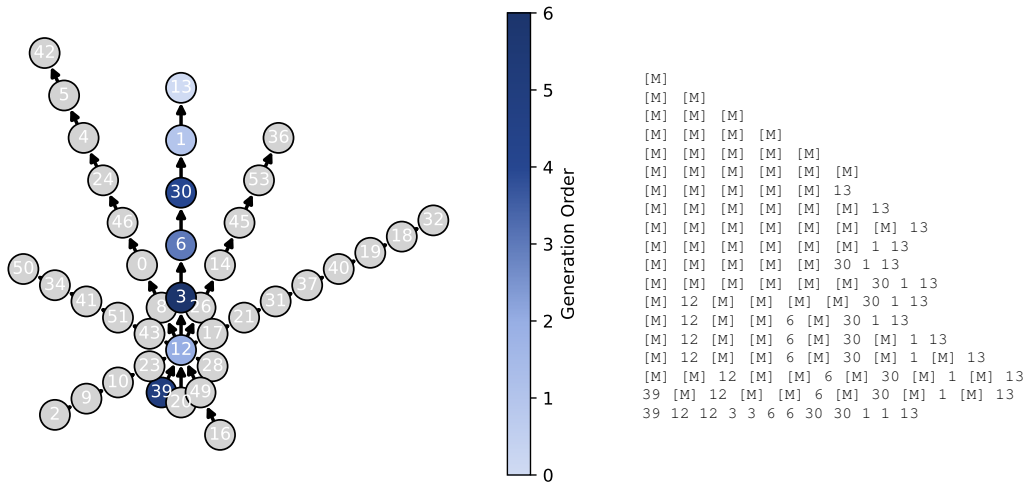


Figure 11. Example of generation order for FlexMDM.

Task	Model	Exact Match (%)	Token Accuracy (%)
star_medium	ARM	75.0	81.4
	MDM	36.5	90.6
	FlexMDM		
	(conf=null)	89.6	95.7
	(conf=top_prob)	91.3	97.0
	LFlexMDM (Aux. Size=small)		
	(b_um=1, conf=null)	93.2	97.8
	(b_um=1, conf=top_prob)	93.0	97.7
	LFlexMDM (Shared=True)		
	(b_um=1, conf=null)	93.6	97.7
(b_um=1, conf=top_prob)	93.2	97.6	
star_hard	ARM	23.0	43.2
	MDM	21.0	54.9
	FlexMDM		
	(conf=null)	6.0	48.5
	(conf=top_prob)	7.4	49.8
	LFlexMDM (Aux. Size=small)		
	(conf=null)	38.0	64.5
	(b_um=1, conf=null)	87.9	96.3
	(b_um=1, conf=top_prob)	88.1	96.7
	LFlexMDM (Shared=True)		
(b_um=1, conf=null)	34.2	66.5	
(b_um=1, conf=top_prob)	69.7	86.9	

Table 6. Raw results for star graph traversal tasks.

G. Related Work

Discrete Flow Matching and Stochastic Interpolants Developed in quick succession by [Campbell et al. \(2024\)](#) and [Gat et al. \(2024\)](#), Discrete Flow Matching (DFM) extends the generative framework of continuous Flow Matching (FM) ([Lipman et al., 2022](#)) to discrete and general probability spaces. For DFM as for FM, the training objective is to learn the velocity field (used for sampling) which generates a probability path that interpolates between coupled distributions, most commonly between noise (p_0) and data (p_1 or p_{data}). Unlike the time-dependent continuous velocity vector field in Continuous Normalizing Flows (CNFs) ([Chen et al., 2018](#)), the velocity field for DFM is presented as the time-dependent rate matrix within a Continuous Time Markov Chain (CTMC) realization ([Campbell et al., 2024](#)) which transports samples through a continuum of marginal distributions $\{p_t\}_{t \in [0,1]}$ with $p_{t=1} = p_1$. Connected to the rate matrix by the Kolmogorov Forward Equation (KFE), these marginals bridge p_0 and p_1 in finite time and form a stochastic process formalized as stochastic interpolants by [Albergo et al. \(2023\)](#).

Diffusion with Learnable Noise The standard diffusion approach from DDPM ([Ho et al., 2020](#)) uses an isotropic Gaussian noising kernel for the forward process, which gives a closed-form expression for the marginal and guarantees that the functional form of the learnable posterior is likewise an isotropic Gaussian. Despite the simple and effective formulation, the reverse noising process is independent over positions and has no explicit mechanism by which to coordinate denoising decisions among positions or pixels. Moving away from standard Gaussian noising, [Bansal et al. \(2023\)](#) show that the generative abilities of image diffusion models are not strongly dependent on the the corruption process, while [Daras et al. \(2022\)](#) learn the score function for any linear corruption process. Both [Rissanen et al. \(2022\)](#) and [Hoogeboom & Salimans \(2022\)](#) introduce diffusion based on blurring or heat dissipation, where the noise process destroys low-information regions faster than high-information ones, thus instilling a coarse-to-fine inductive bias into the generative process. MuLAN ([Sahoo et al., 2024b](#)) also introduces a multivariate per-position *learned* noise schedule, tightening the variational ELBO and allowing diffusion to denoise different spatial regions at different rates. Even more recently, [Bartosh et al. \(2024\)](#) propose Neural Flow Diffusion Models (NFD) which defines the forward process’ conditional SDE via a learnable parametric transformation and enables the specification of a variety of data- and time-dependent noising processes.

Similarly to image diffusion, the prevailing framework in widely-adopted masked diffusion models ([Shi et al., 2024](#); [Sahoo et al., 2024a](#)) relies on the reversal of a non-parametric masking schedule that is independent and uniform across positions. However, this paradigm does not take into account the potential value of learning which token positions to decode in what order. [Wang et al. \(2025\)](#) take up this question of token generation ordering.

Variable Length Discrete Flow Matching The useful desiderata of *i*) modeling distributions over variable-length sequences and *ii*) the ability to insert tokens have inspired a number of recent works to move away from fixed-window text diffusion towards insertion- and substitution- based discrete flow models in which positions during the generation process acquire a relative rather than absolute interpretation. In particular, FlexMDM ([Kim et al., 2025a](#)) grows a sequence by parameterizing an action space which allows the insertion of a mask token and the unmasking of already-inserted masks. Concurrently with FlexMDM, EditFlows ([Havasi et al., 2025](#)) defines a discrete flow by means of insertion, deletion and substitution operations to support variable-length sequence generation. ([Patel et al., 2025b](#)) proposes insertion language modeling (ILM) which allows the direct insertions of unmasked tokens, as opposed to the two-step insertion/unmasking approach of FlexMDM.

Table 7. Full set of results for *de novo* small molecule generation. For both FlexMDM and LFlexMDM, we use 1024 sampling steps. * indicates frozen, 🔥 indicates trainable; ✓/✗ indicates whether confidence-based position selection for unmasking is enabled, and p indicates the truncation threshold for nucleus sampling (Holtzman et al., 2020). † Noutahi et al. (2024) ‡ Lee et al. (2025)

Model				Validity (%)	Diversity	Uniqueness (%)	Quality (%)
b_{um}	b_{in}	conf.	p				
SAFE-GPT [†]				94.0 ±0.4	0.879 ±0.001	100.0 ±0.0	54.7 ±0.3
MDM [‡]				96.7 ±0.3	0.896 ±0.001	<u>99.3</u> ±0.2	53.8 ±1.7
FlexMDM							
*	*	×		98.9 ±0.4	0.922 ±0.001	96.4 ±0.3	39.5 ±1.6
*	*	✓		86.5 ±1.8	0.906 ±0.004	20.2 ±1.5	5.8 ±0.8
LFlexMDM (Aux. Size=medium)							
*	🔥	✓	1.0	98.9 ±0.2	<u>0.921</u> ±0.001	95.6 ±0.5	39.6 ±2.3
*	🔥	✓	0.9	99.7 ±0.2	0.909 ±0.001	95.0 ±0.8	49.3 ±1.7
*	🔥	✓	0.5	99.7 ±0.1	0.870 ±0.002	88.6 ±0.5	54.7 ±1.7
*	🔥	✓	0.2	<u>99.8</u> ±0.1	0.857 ±0.001	86.1 ±0.7	59.2 ±1.1
*	🔥	×	1.0	99.0 ±0.2	<u>0.921</u> ±0.001	96.1 ±0.9	39.1 ±1.9
*	🔥	×	0.9	99.5 ±0.1	0.909 ±0.001	95.5 ±0.5	50.0 ±0.4
*	🔥	×	0.5	99.3 ±0.3	0.889 ±0.002	93.0 ±1.0	46.9 ±1.0
*	🔥	×	0.2	99.6 ±0.2	0.887 ±0.002	90.9 ±0.7	46.8 ±1.5
LFlexMDM (Aux. Size=small)							
*	🔥	✓	1.0	99.0 ±0.2	0.919 ±0.001	95.9 ±0.5	43.8 ±0.8
*	🔥	✓	0.9	99.7 ±0.1	0.902 ±0.001	95.7 ±1.2	57.5 ±2.8
*	🔥	✓	0.5	99.7 ±0.1	0.837 ±0.003	82.6 ±0.7	52.4 ±1.7
*	🔥	✓	0.2	99.9 ±0.1	0.830 ±0.004	79.1 ±1.0	50.1 ±0.9
*	🔥	×	1.0	98.9 ±0.5	0.918 ±0.001	96.4 ±0.7	43.5 ±1.3
*	🔥	×	0.9	99.5 ±0.2	0.904 ±0.002	96.7 ±0.7	55.0 ±1.4
*	🔥	×	0.5	99.6 ±0.2	0.878 ±0.002	92.2 ±0.9	<u>61.2</u> ±1.8
*	🔥	×	0.2	99.5 ±0.2	0.864 ±0.002	87.2 ±1.3	62.1 ±1.7
LFlexMDM (Aux. Size=xtiny)							
*	🔥	✓	1.0	99.4 ±0.3	0.919 ±0.001	96.3 ±0.4	43.1 ±1.8
*	🔥	✓	0.9	99.7 ±0.2	0.902 ±0.001	96.0 ±1.0	57.8 ±1.1
*	🔥	✓	0.5	99.7 ±0.1	0.851 ±0.003	87.8 ±1.2	60.0 ±0.4
*	🔥	✓	0.2	99.9 ±0.1	0.834 ±0.003	80.5 ±1.8	56.6 ±1.2
*	🔥	×	1.0	99.0 ±0.2	0.918 ±0.000	97.1 ±0.8	43.0 ±1.4
*	🔥	×	0.9	99.6 ±0.2	0.904 ±0.001	96.4 ±0.7	54.0 ±1.8
*	🔥	×	0.5	99.7 ±0.2	0.881 ±0.002	93.8 ±0.7	57.5 ±0.8
*	🔥	×	0.2	<u>99.8</u> ±0.1	0.876 ±0.002	90.3 ±1.5	58.9 ±1.2
LFlexMDM (Shared Backbone)							
🔥	🔥	✓	1.0	98.6 ±0.5	0.920 ±0.001	95.7 ±0.5	39.9 ±1.6
🔥	🔥	✓	0.9	99.4 ±0.3	0.905 ±0.001	95.8 ±0.5	53.7 ±1.4
🔥	🔥	✓	0.5	99.6 ±0.1	0.851 ±0.001	82.5 ±1.1	59.0 ±1.4
🔥	🔥	✓	0.2	99.7 ±0.1	0.844 ±0.003	80.5 ±1.0	58.5 ±1.8
🔥	🔥	×	1.0	98.4 ±0.4	0.920 ±0.001	96.7 ±0.5	41.5 ±1.7
🔥	🔥	×	0.9	98.9 ±0.3	0.905 ±0.001	95.2 ±1.4	52.1 ±0.5
🔥	🔥	×	0.5	99.1 ±0.3	0.880 ±0.003	90.8 ±0.8	57.6 ±1.7
🔥	🔥	×	0.2	99.0 ±0.6	0.868 ±0.002	88.1 ±1.3	61.1 ±0.9